

Carbon Flux from Wood Bioenergy Subsidies: A Structural Model of Forest Land Use

[[Click here for latest version](#)]

Benjamin Rommelaere*

October 29, 2025

Abstract

Wood bioenergy offers one path to reduce carbon emissions from fossil energy and has become an important energy source in the U.K. and EU-27, driven largely by subsidies. At the smokestack, burning wood emits more CO₂ than coal, so any climate benefit depends on its impact on forest carbon flux. I study the effects of these subsidies on forests in the U.S. South, the world's main export region of wood bioenergy, to assess whether they have delivered climate benefits. I develop a dynamic structural model which unifies land use and harvesting decisions while incorporating local oligopsony power of mills over landowners. The model is estimated on a panel of 5.1 million land plots built from remote sensing data on land use, tree harvesting, and forest biomass accumulation. The results show most exported wood comes from new harvests without offsetting increases in planting rates, leading to net deforestation, lower forest carbon stocks, and reduced annual carbon sequestration. The impact is substantial: in 2024, the estimated loss in annual sequestration equals 1.4 percent of U.K. emissions, and by 2050 the social cost of the lost forest carbon reaches \$53 billion. What looked bad at the smokestack is worse once the forest response is measured. Spatial variation in the results suggests that location-based sourcing restrictions could reverse this result and deliver climate benefits.

*Department of Economics, University of Toronto, Toronto, Canada, b.rommelaere@mail.utoronto.ca
I am deeply indebted to my advisors Eduardo Souza-Rodrigues, Victor Aguirregabiria, and Stephan Heblich for their thoughtfulness and generosity throughout this project. I am grateful for the detailed comments from all participants of the University of Toronto Climate Economics Seminar and IO Brownbag workshops, with special thanks to Robert McMillan, Jeffrey Sun, Christoph Semken, Peter Morrow, and Mitsuru Igami. I gratefully acknowledge the Social Sciences and Humanities Research Council of Canada (SSHRC) and the Center for Climate Positive Energy at the University of Toronto for their generous funding; and the Department of Economics at the University of Toronto for its generosity in supporting data acquisition costs.

1. Introduction

Wood bioenergy offers one pathway to reduce global emissions and has received substantial subsidies under implicit assumptions of carbon benefits. It is also an important renewable fuel in Europe, where EU and U.K. subsidies have increased use since the EU-28's Renewable Energy Directive (RED-I) in 2009. By 2020, the original end date for RED-I, the EU-27 received 30% of its renewable energy supply from wood, while the U.K. generated 8% of its electricity supply from wood (Department for Energy Security and Net Zero, 2025; European Commission, 2024).¹ Yet wood remains a controversial fuel to subsidize due to the complex atmospheric carbon implications of increased usage.

The main source of controversy is in the substantial smokestack emissions which are roughly 20 percent higher than coal per unit of energy produced. This means that wood bioenergy yields climate benefits only when subsidies do not cause new harvests and instead promote increased use of decaying waste wood, or when any new harvests are fully replanted so that resulting carbon debt is gradually repaid through forest regrowth. In practice, however, replanting is often imperfect, and even small losses in forested area can lead to large and persistent forest carbon losses. As climate goals require steep near-term emission reductions, understanding the pace and completeness of forest carbon recovery is critical. Ultimately, the climate impact of wood bioenergy subsidies depends on how landowners adjust their harvesting, replanting, and land use decisions in response to these subsidies. Yet official carbon accounts remain too coarse to reveal whether, or when, the carbon debt is ever repaid.

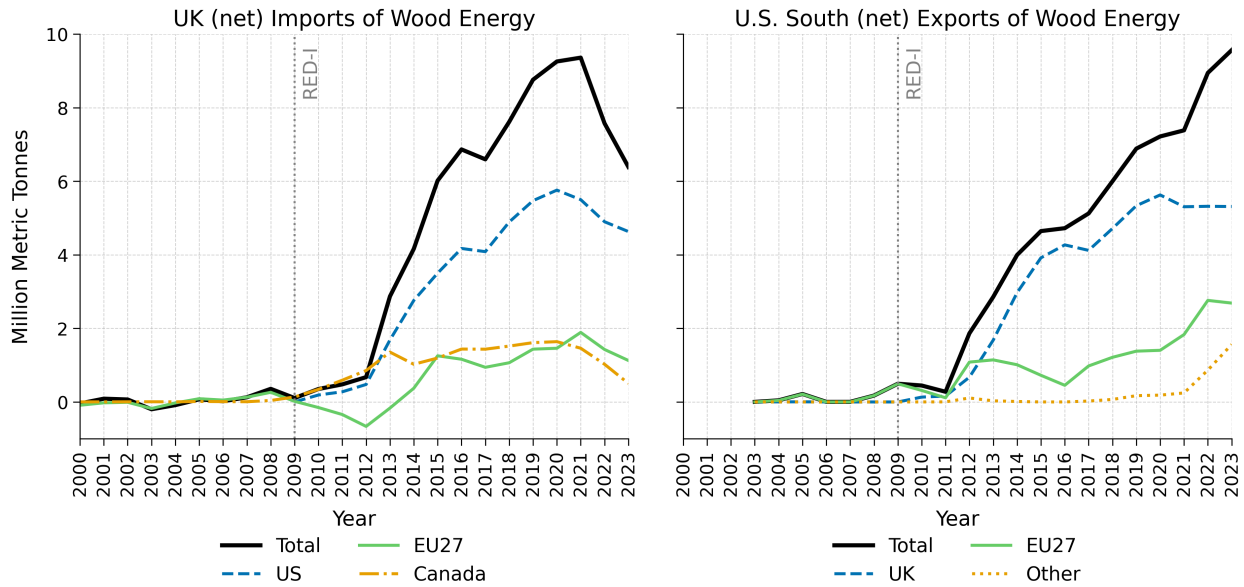
Determining where the marginal unit of wood comes from further complicates the carbon accounting. Even when bioenergy firms report sourcing directly from waste wood, these materials may have otherwise supplied other buyers, causing them to substitute toward new harvests. As a result, feedstock data alone cannot reveal whether increased bioenergy demand draws from existing waste streams or induces additional forest harvests. Identifying the true source of the marginal unit therefore requires understanding how markets as a whole respond to subsidies.

This paper provides empirical evidence on these market-level adjustments. It estimates how landowner harvesting, replanting, and land use decisions respond to bioenergy subsidies to identify where the marginal unit of wood is supplied from and how these responses affect the forest carbon sink over time. Together, these results provide a basis for evaluating the true carbon consequences of bioenergy policies.

¹U.K. electricity generation data comes from U.K. Dukes Table 6.2 and refers to plant biomass, which is predominantly wood-based biomass.

The analysis examines how landowners responded to the surge in bioenergy demand created by RED-I subsidies. These subsidies caused wood bioenergy demand to exceed domestic supply, generating sustained import demand. Figure 1 illustrates the resulting change in international trade for the U.K., Europe's largest importer, and the U.S., the primary global exporter of wood bioenergy. Prior to RED-I, trade in wood energy was minimal; afterwards, it expanded rapidly, especially from the U.S. South, which emerged as the world's leading exporter. The U.S. South in turn provides an ideal setting to study the effects of RED-I subsidies on landowner behavior, as the effect of the subsidies can be identified from the entry of new export-oriented wood bioenergy mills.

Figure 1: Wood Bioenergy Trade



Source: UK import data is from Eurostat HS4 trade data (4401: Fuel Wood), while U.S. export data source is from U.S. Import & Export Merchandise Trade Statistics, Port-level HS6 data (440131: Wood Pellets). Exports from southern ports calculated by author.

The structure of the forestry market guides my modeling decisions and provides the means by which landowner choices respond to changes in bioenergy policy. Each forest plot is of a given wood type, hardwood or softwood, and each type is sold to distinct sets of mills that purchase only that wood type, creating two largely separate markets for wood. A harvested tree yields multiple products: high-grade sawlogs, lower-grade fibre logs, and residual waste wood. Landowners sell the trees at auction to determine the actual price for their wood. Since wood is a globally traded commodity and bioenergy remains a small share of total demand, bioenergy subsidies do not empirically pass through to the average market prices paid to landowners. However, the market structure provides another mechanism through which landowner behavior is affected.

Because logs are bulky and expensive to transport, landowners sell to a small number of nearby mills, resulting in localized oligopsony markets. The number and composition of these mills determine local competition and therefore the expected returns to harvesting and tree planting. This structure also provides a natural way for changes in the set of wood buyers to affect landowner behavior. The number of local buyers shifts the potential bidder set, and thus long-run expected prices, which in turn affects decisions.

Landowners face a forward-looking decision problem. Planting trees requires upfront land-preparation and planting costs that only pay off decades later at harvest, while converting land to alternative uses such as agriculture or development also involves significant fixed costs. These features make land-use and harvest choices dynamic. I incorporate this logic into a dynamic discrete choice model that jointly captures harvesting, planting, and land-use decisions. In each period, landowners with forests decide whether to harvest the standing biomass or allow the current forest to continue growing. If they delay harvest, both the expected biomass and the composition of high-, low-, and waste-grade wood evolve. If they harvest, they receive profits from the sale of biomass at market prices net of local markdowns. After harvest, landowners begin the next period with bare land and must choose whether to replant trees or switch to their best alternative use. Landowners in nonforest uses receive payoffs that depend on land characteristics, such as proximity to urban centres and agricultural suitability, while transitions into forestry require fixed planting costs.

I estimate the model using high-resolution spatial data that track land use, forest loss, fires, and aboveground biomass, combined with information on forest type, disturbance risk, urban proximity, agricultural suitability, and local market structure. These data allow me to characterize both the ecological and economic environments in which landowners operate.

Using the estimated model, I simulate harvest behavior, biomass accumulation, and carbon flux from the start of RED-I through 2050 under observed conditions with bioenergy mills. I then construct a counterfactual that removes wood bioenergy mills, which alters local markdowns and expected returns to harvesting and replanting. By comparing these two simulations, I obtain an estimate of the induced harvests and impact on forest carbon flux due to RED-I subsidies.

The results show that nearly all of the wood required to match observed U.S. bioenergy production is supplied through increased harvesting rather than waste wood. This contrasts with feedstock reports suggesting that only 10–20 percent of bioenergy production comes directly from harvested logs. The difference arises from market substitution: as bioenergy mills increase demand for waste wood, other fibre-consuming mills shift toward using newly

harvested logs.² This pattern is consistent with U.S. Forest Service (USFS) data showing that the main form of waste wood, sawdust, was already over 99 percent utilized prior to RED-I (Johnson et al., 2011). These findings imply that most subsidized wood bioenergy is sourced from new harvests, and that realizing climate benefits depends on whether and when the resulting carbon debt is repaid through forest regrowth.

To assess this, I compare predicted biomass accumulation and carbon flux under observed conditions with bioenergy mills to a counterfactual in which these mills are absent. While forests in both scenarios continue to act as a global carbon sink, the model implies substantially slower biomass accumulation in the presence of bioenergy demand. By 2024, the model implies that annual carbon sequestration was roughly 5 million metric tonnes less than it would have been in the absence of wood bioenergy mills, equivalent to 1.4% of U.K. emissions. Through 2050, this results in a social cost of loss forest carbon of \$53 billion (2020 USD). The model further predicts that carbon sequestration remains persistently lower with bioenergy over any relevant planning horizon. In short, what looked bad for the climate at-the-smokestack looks substantially worse in the forest. Even with carbon capture and storage at bioenergy plants, atmospheric CO₂ would continue to rise due to the loss of forest carbon stock.

This result contrasts with current literature on wood bioenergy policies, which show a simulated increase in carbon stocks or contemporaneous carbon balance (Abt et al., 2014; Aguilar et al., 2022). The key difference is that this paper allows for imperfect replanting which, as revealed by the data, leads to additional net land use switching post harvest which is not offset by increased replanting or new forest establishment. As a result, the model estimates a cumulative loss of roughly 1,500 km² of forest area by 2050, comparable to the size of Orlando's urbanized area.

This decline in forest area drives the persistent reduction in carbon sequestration. Our results also show that in the short run, landowners lower their harvest rate in anticipation of higher future prices. The model also captures short-run dynamics in which landowners temporarily reduce harvest rates in anticipation of higher future prices, potentially explaining why short panels show contemporaneous carbon balance. A distinguishing feature of this framework is that it explicitly tracks the evolution of forest carbon over time, allowing direct measurement of how bioenergy demand alters long-run carbon flux. In contrast, prior studies rely on static general equilibrium approaches that infer supply elasticities from short-run price variation and assume perfect replanting rates.

These decline in forest area and the resulting carbon losses are not uniform or inevitable.

²It also reflects accounting issues in feedstock data, whereby minimally processed wood handled on-site is classified as waste rather than as new harvests.

The high spatial resolution of the data and the rich structure of the model allow decomposition of the results by observable landscape characteristics. This shows that most carbon losses are concentrated in hardwood forests and areas with high agricultural or urban development value, while softwood forests in low-value areas exhibit modest carbon gains. The spatial heterogeneity suggests that the overall carbon effect of bioenergy policy depends on which forests wood are sourced from. Consequently, existing policy frameworks such as the EU Deforestation Regulation (EUDR) and the U.K.’s forthcoming Forest Risk Commodity Regulation could integrate spatial sourcing criteria to better target low-agricultural-value softwood regions and restrict sourcing from areas with high-development pressure and hardwood forests. Incorporating spatial targeting these deforestation laws could ensure that renewable energy policies deliver genuine carbon benefit.

The remainder of the paper proceeds as follows. Section 2 reviews related literature. Section 3 provides background on wood bioenergy policies and an overview of the forestry industry in the U.S. South. Section 4 introduces an expository carbon accounting framework that highlights the conditions required for bioenergy to deliver climate benefits. Section 5 describes the data and presents descriptive evidence that motivates the model and counterfactual design. Section 6 develops the dynamic model, and Section 7 discusses its estimation. Section 8 presents the counterfactual simulations and results. Section 9 concludes.

2. Related Literature

This paper relates to several strands in the literature. Most directly, it connects to a growing literature using dynamic discrete choice models to study land use and environmental policy (Scott, 2014; Sant’Anna, 2024; Araujo et al., 2025; Hsiao, 2025). These papers typically examine how biofuel subsidies or agricultural policies affect land use and deforestation-related emissions by modeling long-run price changes and allowing landowners to convert forest to nonforest land subject to switching costs. Closest to this paper is Sant’Anna (2024), though I analyze a different policy context that leads to forest expansion rather than loss. The paper is further related to Araujo et al. (2025), who estimate total forest carbon responses to environmental policy using a similar dynamic framework but in a distinct industrial setting. I build on this work by modeling the inverse problem: wood bioenergy subsidies that raise the value of forested land and cause transitions into forestry. I also introduce a novel interaction between buyer concentration and landowner behavior by embedding markdowns directly in the discrete choice framework.

A second strand of literature develops structural models of forestry and harvest behavior using dynamic methods. This work originates with the capital-theoretic rotation model of

Faustmann (1849), extended to stochastic settings by Provencher (1995a,b), who show that unobserved yield shocks explain much of the variation in harvest timing. Wu et al. (2022) apply a similar framework to forest management in China, while Guo and Costello (2013) and Hashida and Lewis (2019) extend it to incorporate climate and species dynamics. My paper is closely related to Rust and Paarsch (2020), who model harvest timing as a function of detailed spatial cost heterogeneity. I extend this approach to an estimable framework at a continental scale and unify the extensive (land use) and intensive (harvest timing) margins within a single dynamic discrete choice framework that incorporates market power, imperfect replanting, and landowner amenity preferences following Hartman (1976).

This paper also contributes to the literature on timber market auctions showing how competition, information, and market structure shape price formation (Baldwin et al. (1997), Athey and Levin (2001), Haile (2001), Li and Perrigne (2003), Athey et al. (2011), Préget and Waelbroeck (2012), Kuehn (2019)). This literature shows that collusion and low participation suppress bids, while transparency and open formats raise revenues by intensifying competition. More recent work highlights how bidder identity and downstream concentration create externalities that distort prices and allocation. I incorporate these insights in a novel way by embedding buyer concentration directly within the dynamic land-use model, linking local auction competition to long-run landowner behavior.

Finally, this is not the first paper to study the impacts of RED-I subsidies on the U.S. South wood forestry industry. Abt et al. (2014) and Duden et al. (2023) use partial-equilibrium simulations and find that increased bioenergy demand raises harvests and prices while maintaining or increasing long-run forest carbon, though their results hinge on assumed elasticities and perfect replanting. Williams and Xi (2021) documents higher harvest rates and declining forest cover in sourcing regions but lacks causal identification. Aguilar et al. (2022) use a matched difference-in-differences approach and find near-term carbon neutrality but does not allow for land use adjustment and imperfect replanting. Last, Parajuli et al. (2024) estimate a staggered difference-in-differences model at the market level and find no significant price or quantity effects, but their design ignores spatial spillovers, biasing estimates toward zero. Relative to these studies, I develop a dynamic structural model that microfounds land-use and harvesting behavior to recover the causal effect of bioenergy demand on forest carbon outcomes.

3. Background

Policy Setting The European Union’s Renewable Energy Directive (RED-I), enacted in 2009, was the first major policy to subsidize wood bioenergy as part of its decarbonization

agenda. The inclusion of wood as a renewable energy source has been controversial because combustion emits more greenhouse gases at the smokestack than coal or natural gas.³ Under RED-I, member states were required to submit National Renewable Action Plans (NRAPs) detailing how they would meet their 2020 renewable-energy targets. Most had implemented incentives for renewable energy by 2011, with several starting earlier.

While wood bioenergy was a significant energy source prior to RED-I, mainly in residential heating, its use expanded substantially following the directive's implementation. After RED-I, member states began to subsidize wood bioenergy both in residential heating and large-scale electricity generating facilities. Member states, such as Italy, France, and Germany, subsidized small-scale biomass stoves and boilers; while others, such as the Netherlands, Denmark, and the U.K., subsidized co-firing biomass in coal facilities. In both cases, wood pellets are the preferred fuel due to their low moisture content, uniform size, increased efficiency, and lowered trade costs for bulk international shipping. The scale of biomass energy subsidies explains the increase in supply from this energy source. Annual subsidies for all forms of biomass in the EU-27 have ranged from \$9-\$20 billion, similar in scale to subsidies for wind, and about two-thirds of subsidies for solar energy (European Commission, 2021).⁴

Within this total, exact national spending on wood bioenergy is difficult to isolate, as subsidies target solid biomass for heat or electricity, and agricultural and wood-based biomass fuels are largely fungible in energy production. For solid biomass used in electricity generation, predominantly wood pellets, subsidies have ranged from roughly \$5–\$5.5 billion across the EU-27 (Smith et al., 2022). In the U.K., annual subsidies for co-firing wood have totaled \$1.0–\$2.2 billion, about half the level of wind subsidies and twice that of solar (Smith et al., 2022; UK National Audit Office, 2025). These programs drove the conversion of coal plants to biomass and enabled the full coal phase-out by 2024. These subsidies are in addition to the exemptions from carbon taxation on smokestack emissions from burning biomass, which are substantial given the fuel's low efficiency. For example, U.K. wood-pellet combustion has accounted for 2–4 percent of national greenhouse gas emissions since RED-I. In 2020, exemptions from the EU Emissions Trading System (ETS) equated to approximately \$1 billion in the U.K., while across the EU-27 the corresponding exemption equated to nearly \$11 billion.⁵

³Wood pellets in particular produce roughly 1.2 times the amount of GHG's per joule than coal, and more than 2 times the GHG's of natural gas.

⁴The EU Emissions Trading System also exempts biomass fuels from carbon taxation which may have increased usage in some industries; but, due to low carbon prices in the 2005–2009 period, the impact was much more limited than the direct supports put in place by member countries after RED-I was passed.

⁵Authors calculations. Pellet usage in the EU-27 and U.K. come from USDA Wood Pellet Annual reports, which are converted to CO₂ emissions using the official EU smokestack conversion factor. These are then valued using the average annual ETS auction value in 2024.

These subsidies caused demand for wood bioenergy to exceed domestic supply in many member states, leading to large imports of wood pellets. This is especially true in the U.K., which became Europe's largest importer of wood energy.⁶ Figure 1, illustrates how this excess demand was met almost entirely by exports from the U.S. South, which supplied nearly 99% of all U.S. pellet exports after RED-I. Prior to the policy, U.S. wood pellet exports were effectively zero, and expanded sharply after 2011 as NRAP's were implemented, highlighting how European policy directly restructured U.S. wood markets.

By 2020, RED-I's EU-wide 20% target was achieved. However, this was largely due to wood burning: 30% of EU-27 renewable energy consumption in 2020 was from wood-based biomass products (European Commission, 2024). In the UK, which predominantly subsidized wood bioenergy in electricity generation, 8.3% of all electricity generated was directly from wood pellets in 2020 (Department for Energy Security and Net Zero, 2025).⁷.

Although RED-I's main policy objectives were achieved by 2020, demand for wood bioenergy is expected to keep growing. Revisions to RED-I in 2018 and 2023 raised the EU's renewable energy targets for 2030 to 32 percent and 42.5 percent, respectively, reinforcing continued reliance on biomass.⁸ Since leaving the EU, the U.K. has followed a similar path under the Climate Change Act, which retained most domestic renewable energy supports.⁹ Together, these policy frameworks continue to favor biomass as a renewable fuel, leading to projected growth in bioenergy demand as part of the region's decarbonization strategy (European Commission, Joint Research Centre, 2024)

Industry Background Over 90 percent of land in the U.S. South is privately owned, with forests accounting for about half of the total land area. Forest cover has declined steadily since the early 1990s, largely driven by urban expansion (Wear and Greis, 2013). Various levels of government own 14% of forested land. While public forests are often restricted to remain forested, only a small share of public forests are legally protected from harvest.¹⁰ The remainder of public forests are actively managed for commercial value. Among private

⁶In 2020, the UK accounted for 65% of net imports of wood pellets in the old EU-28. U.K. wood pellets are primarily sourced from the United States, which provided 77% of imports (US Trade Data, 2024, author's calculations).

⁷While the official data is for electricity generation from all forms of plant biomass, the report notes that this category is predominantly wood pellets.

⁸Recent revisions to RED also introduced stricter sustainability criteria, prompting several countries to enact national limits on biomass subsidies (e.g. Netherlands, Slovakia, Portugal), reflecting growing climate compatibility concerns of biomass power.

⁹A 2025 decision introduced a cap to the support for wood pellets, halving subsidies by 2027 and restricting future eligibility to plants demonstrating a credible pathway to carbon capture and storage by 2031.

¹⁰These areas include national parks, wilderness areas, and certain state conservation lands.

owners, individuals and families are the largest ownership group, followed by institutional investors and finally upstream mills.¹¹

Forests in the U.S. South consist primarily of fast-growing softwood plantations and slower-growing hardwood forests. wood from each type is distinct and requires different mill technologies for processing. For a given forest plot, trees yield three separate wood products: sawtimber, pulpwood, and residues. Sawtimber is the portion of the tree trunk that exceeds 12 inches in diameter and is the main feedstock for sawmills.¹² Pulpwood refers to the 4–12-inch portion of the trunk, which supplies fiber-consuming mills. These mills can also substitute pulpwood with sawdust, a byproduct of sawmills. Residues make up the remainder of the tree (i.e. the branches, leaves), and typically do not have commercial value. Residues are considered waste product that is left on site to decay or is removed via burning or disposal.¹³

When selling timber, private landowners typically hire consulting foresters to estimate merchantable volume and obtain market price quotes. Landowners may then negotiate directly with local mills or solicit sealed bids through a first-price auction, often represented by their forester. Recent surveys report that over 90 percent of private timber sales utilize sealed-bid auctions (Grove et al., 2019). The winning bidder pays the landowner in full, net of forester fees, and the purchaser pays for all harvesting and transportation costs. Public timber sales are similarly conducted at auction, using sealed-bid or English formats.

Following a clearcut, landowners may reforest naturally or artificially. Natural regeneration involves leaving selected “seed trees” to repopulate the site, while artificial regeneration requires site preparation and planting nursery-grown seedlings. The majority of softwood forests are replanted artificially, while hardwood forests are more likely to be left to regenerate naturally (Schelhas et al., 2021). If a landowner instead chooses to convert their land to non-forest uses, they must pay additional stump removal and land clearing costs. Harvesting typically occurs in the year of sale, with replanting or conversion decisions taking place the following year.

Mills source wood locally, as raw logs are bulky and costly to ship long distances relative

¹¹Families control approximately 55 percent of forest land although ownership is highly skewed: although 59 percent of family owners hold fewer than 10 acres, over 60 percent of family-owned acreage belongs to owners with more than 100 acres (Caputo and Butler, 2025). Downstream mills own approximately 4% and the remainder of forest land is owned by institutional investors (Sass et al., 2021) Forest ownership structure has changed over time, most notably by the exit of downstream mills which controlled approximately 20% of land in the 1990's (Butler and Wear, 2013).

¹²For softwood forests, it takes approximately 25-30 years for the majority of the trees volume to be sawtimber; for hardwood forests it takes 50-60 years.

¹³Residues may have some value to landowners by contributing to nutrient cycling, soil carbon maintenance, and erosion control, all of which may increase future forest productivity.

to their value. The majority of shipments are via truck to mills within an average distance of approximately 50 miles for softwoods, which is often considered the primary catchment area. Hardwood mills typically have a larger catchment areas of up to 75 miles due to more species-specific mill technology and a higher value-per-ton (Gibeault and Coutu, 2015). These geographic limits mean that any given landowner faces only a small number of potential mill buyers.

When wood arrives at the mill, it is first dried and processed into end-use products. Softwood sawmills are large capital-intensive operations, while hardwood sawmills are smaller and more specialized due to limited and heterogeneous feedstock.¹⁴ Sawmills are technologically specialized and process only one wood type, as production equipment and sawing patterns are not interchangeable across species. Fiber-consuming mills include pulp, plywood, and pellet mills. Pulp mills dominate regional wood-fiber demand and operate at large scale with rigid feedstock requirements, typically processing only one wood type.¹⁵ Plywood and pellet mills are smaller, more flexible, and can substitute between forest types or use residues from logging or sawdust waste from sawmills.

In response to RED-I, pellet mills entered wood markets in the U.S. South to supply the growing European demand for bioenergy. Figure 2, panel (a), shows that capacity of export-oriented pellet mills was effectively zero prior to RED-I but increased sharply thereafter, surpassing 14 million metric tonnes by 2023.¹⁶ As shown in panel (b), pellet mills now account for a significant share of fiber-consuming mill capacity across southern states, representing about 15 percent of total regional wood-fiber processing capacity with considerable spatial heterogeneity. As mills compete locally for feedstock, this aggregated state-level data understates their impact on affected landowners. Importantly, pellet mills represent new entrants into local wood markets, as they are not owned by incumbent firms.

4. Carbon Accounting Framework

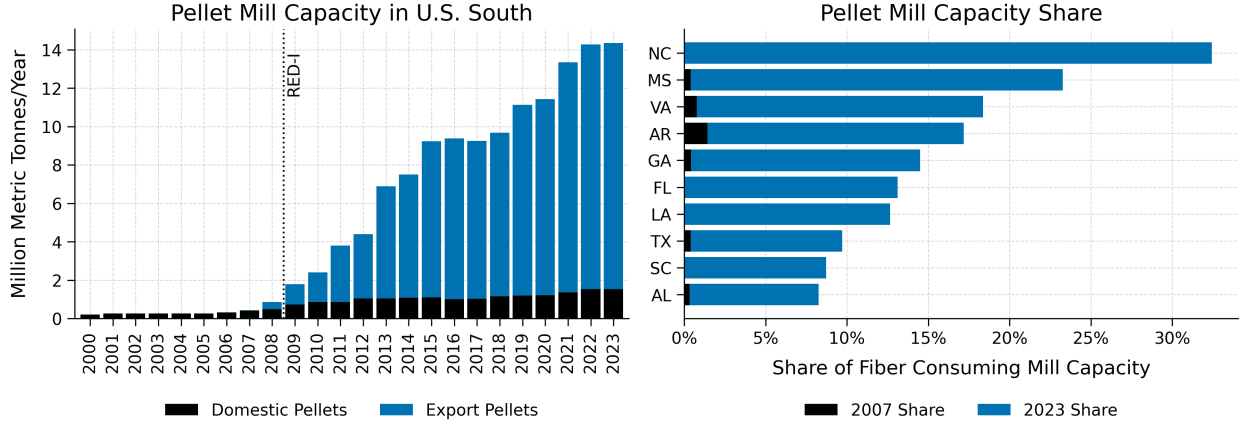
To clarify how wood bioenergy policies affect atmospheric carbon, I introduce a simple accounting identity linking emissions, land use, and fuel displacement. Let A_t denote atmospheric CO₂ in period t , and let total wood bioenergy use be $E_t = H_t + R_t$, where H_t is

¹⁴Hardwood sawtimber takes 50–60 years to mature compared to 25–30 years for softwoods, creating greater spatial dispersion of harvest-ready stands and fewer large mills.

¹⁵Softwood pulp fibers are primarily used in packaging and cardboard, while hardwood pulp is used for tissue and fine paper products. A small number of pulp mills can substitute between wood types based on market conditions, but due to output differences this practice is not common.

¹⁶The initial increase in 2008 reflects the opening of the Cottondale pellet plant in Florida, which began operation in anticipation of RED-I to supply European utilities.

Figure 2: Growth of Pellet Mills



Source: Forisk Mill Database & Southern Environmental Law Center's Pellet Mill Database.

energy from newly harvested wood and R_t is from residues.¹⁷ The policy-induced change in atmospheric carbon is:

$$\Delta A_t = \underbrace{e_b E_t}_{\text{Smoke Stack Emissions}} - \underbrace{\Delta L_t}_{\text{Land Sink}} - \underbrace{e_k E_t}_{\text{Displaced Emissions of Marginal Fuel } k} + \underbrace{\Delta R_t}_{\text{Residue Emissions}} \quad (1)$$

where e_b and e_k are emission factors (tons CO₂ per unit energy) for biomass and the displaced fossil fuel k . The change in forest carbon sequestration between the policy and baseline worlds is captured via ΔL_t , which reflects adjustments in harvesting, land conversion, replanting, and forest growth. Finally, ΔR_t represents the change in emissions from residue decomposition or disposal resulting from the policy. To illustrate the carbon implications for a given biomass policy, I consider two edge cases for the source of E_t : residues and new harvests.

100% Residue Case ($E_t = R_t$). If all bioenergy is sourced from residues, smokestack emissions substitute for decomposition emissions as $e_b E_t = -\Delta R_t$.¹⁸ This simplifies the

¹⁷This includes harvest residues left on site (branches, leaves) and by-products from wood-processing mills. The framework assumes total energy demand is fixed, such that subsidies reallocate energy inputs rather than expand overall consumption. It abstracts from upstream emissions across fuels, assuming these are similar on average. Recent evidence suggests upstream methane leakage from natural gas may be large, narrowing the gap between coal and gas emissions (Howarth, 2024). Upstream emissions per petajoule are higher for wood than for coal (Tran et al., 2023); since coal remains more carbon-intensive than gas, omitting upstream emissions does not alter the main intuition here. Finally, the framework abstracts from differences in forest disturbance risk across harvest frequencies, for which causal evidence remains limited.

¹⁸This simplification assumes residues decompose in the same year as bioenergy combustion and that decomposition has an equal emission factors. In practice, decomposition is heterogeneous. For example, residues are frequently burned on-site (without energy production) releasing carbon immediately while significant shares are left to slowly decay over decades. Further, a share (5–20%) of the decomposing carbon can be stabilized long-term in soils as organic matter. Thus, wood bioenergy front loads emissions, and creates potentially larger emissions than decomposition. Accounting for a decomposition emission lag and

above identity to: $\Delta A_t = -\Delta L_t - e_k E_t$. With no new harvesting, the land sink is left to continue growing; but, landowners may still respond by planting new trees, meaning $\Delta L_t \geq 0$. Displaced fossil emissions are non-negative, implying $e_k E_t \geq 0$. Therefore, residue-based bioenergy is at worst carbon-neutral and can reduce atmospheric CO₂ if forest growth or fossil-fuel displacement effects are positive.

100% New Harvest Case ($E_t = H_t$). When all bioenergy is sourced from new harvests carbon neutrality is harder to achieve as $e_b > e_k$ because wood emits more CO₂ per unit of energy than fossil fuels, and harvests generate additional residues, meaning $\Delta R_t > 0$. Now, carbon neutrality requires the land sink to increase by more than the combined increase in smokestack and residue emissions:

$$\Delta L_t > (e_b - e_k)E_t + \Delta R_t.$$

As smokestack emissions occur immediately while forest regrowth is gradual, harvested bioenergy creates an initial carbon debt repaid only if the forest carbon sink, or forest carbon sequestration, offsets these losses.

The contrast between these edge cases highlights a key empirical question: how much of observed bioenergy use is sourced from new harvests versus residues. Figure 3 shows that U.S. EIA data attributes only 10–20% of pellet feedstock to direct harvests, with the remainder classified as residues. However, the EIA’s data classifications obscure the actual market response. First, wood chips are counted as waste wood but represent minimally processed harvested trees to reduce shipping costs. Second, sawdust is shown to be commonly used by pellet mills but was estimated to be fully utilized prior to the arrival of pellet mills (Johnson et al., 2011). In other words, the EIA data does not account for potential feedstock substitution across competing mills. True harvest increases will therefore exceed reported shares from the EIA feedstock data. To understand the full market-level response accounting for feedstock substitution across mills, we need an estimate of what would have been harvested if pellet mills never entered. This is a key contribution of this paper as the structural model presented below can explicitly calculate the level of market-wide harvests absent pellet mills.

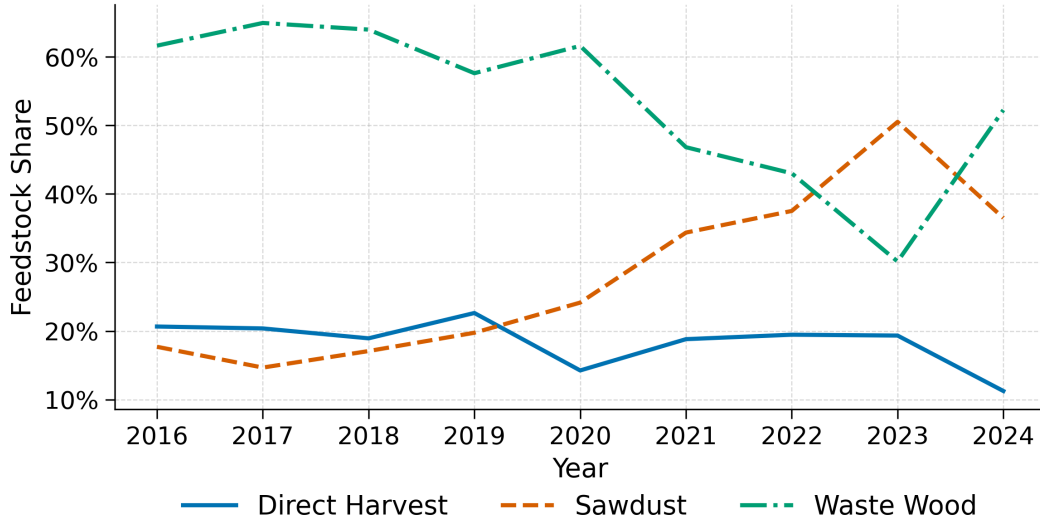
Over a given planning horizon T , cumulative atmospheric CO₂ declines only if:

$$\sum_{t=1}^T \Delta A_t \leq 0 \quad \Rightarrow \quad \sum_{t=1}^T \Delta L_t > \sum_{t=1}^T [(e_b - e_k)E_t + \Delta R_t].$$

Equivalently, any early losses in the land sink, i.e. $\Delta L_t < 0$, must be fully offset by T ,

soil-carbon storage would only reinforce the conclusion presented here.

Figure 3: Pellet Mill Feedstock Shares, U.S. South



Source: EIA Form 63C, Table 3. Shares computed by author. Waste wood includes wood product manufacturing waste, bark, logging residues, wood chips, post-consumer wood, unmerchantable wood, and other wood waste.

meaning the carbon debt must be repaid. As the impact of wood bioenergy policies on L_t is an empirical question, a central contribution of the paper is providing a defensible estimate of this parameter.¹⁹

5. Data & Descriptive Statistics

This paper constructs a novel, spatially explicit dataset linking annual land use, forest biomass, and timber market conditions across the U.S. South. The data combine 30-meter remote-sensing products, including USFS Landscape Change Monitoring System (LCMS) for land use, Global Forest Watch (GFW) for forest loss, and eMapr Forest Biomass Density for aboveground biomass—with species distribution maps (Williams et al., 2020) and remotely sensed cost shifters including slope, insect and disease risk, and site accessibility.²⁰ This dataset allows each 30m by 30m plot of land to be followed through time as forests are harvested, planted, or converted, enabling an analysis of land-use dynamics and market interactions at a scale and sampling resolution not possible with traditional inventory data.

LCMS land-use classes are re-categorized into forest and non-forest after excluding pre-

¹⁹This condition is unchanged if carbon capture and storage is introduced, unless capture rates for biomass substantially exceed those for fossil fuel.

²⁰Appendix A describes data sources, variable construction, and the temporal alignment of decision and biomass data.

existing urban areas, wetlands, and open water.²¹ Forest-loss events are cross-referenced with GFW and LCMS attribution data to separate clearcuts from natural disturbances such as fire or wind damage. The final sample covers roughly one billion 30-m plots across twelve southern states.

Figure 4 shows the study area and land use categories in the year 2000 highlighting the areas excluded from the analysis. Table 1 summarize land-use dynamics between 2000 and 2023. Forest cover declined by about one percentage point overall, reflecting substantial simultaneous afforestation and deforestation. Roughly 4.3 percent of forests present in 2000 converted to non-forest uses, while only 9 percent of previously non-forest plots afforested, yielding a net loss in forest area. This gradual erosion of forest cover aligns with the known trend in the region of urban expansion reducing forest area over time (Wear and Greis, 2013).

Figure 4: Study Region

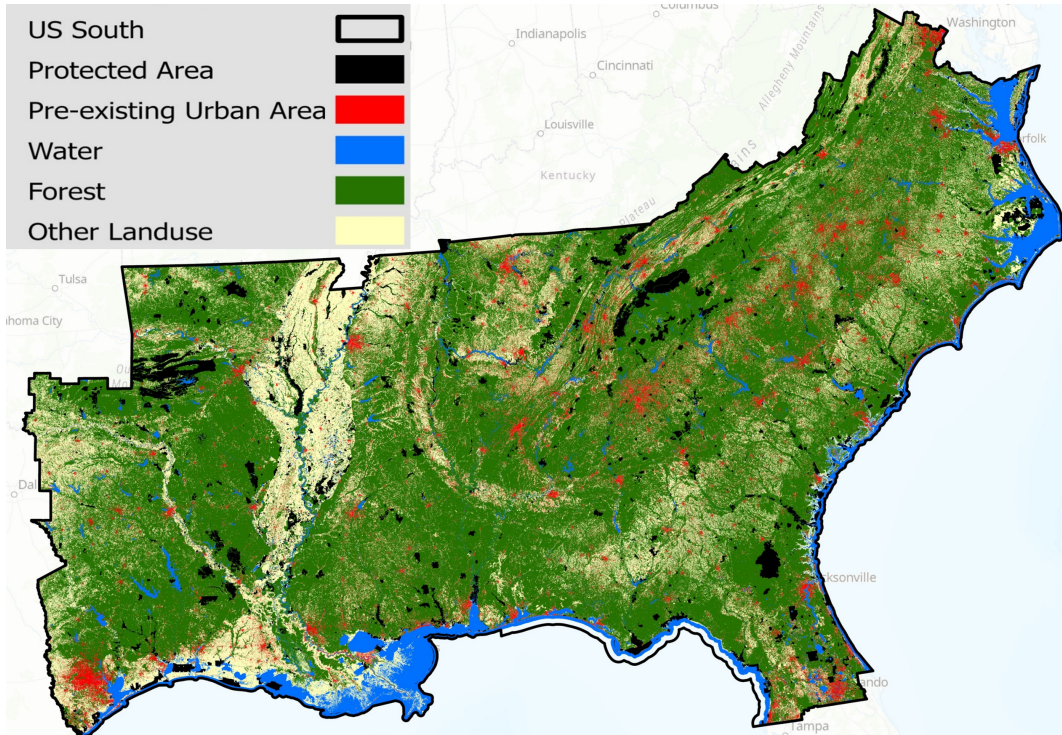


Figure 5 plots annual harvest probabilities by on-site biomass for softwood and hardwood forests. Harvest likelihood rises with biomass and peaks around 17 tons for replanted plots, while land conversion events are concentrated on poorly stocked sites with less than 5 tons of biomass. Softwood stands are harvested and replanted roughly twice as often as hardwoods, but hardwood forests are substantially more likely to be cut and permanently converted at

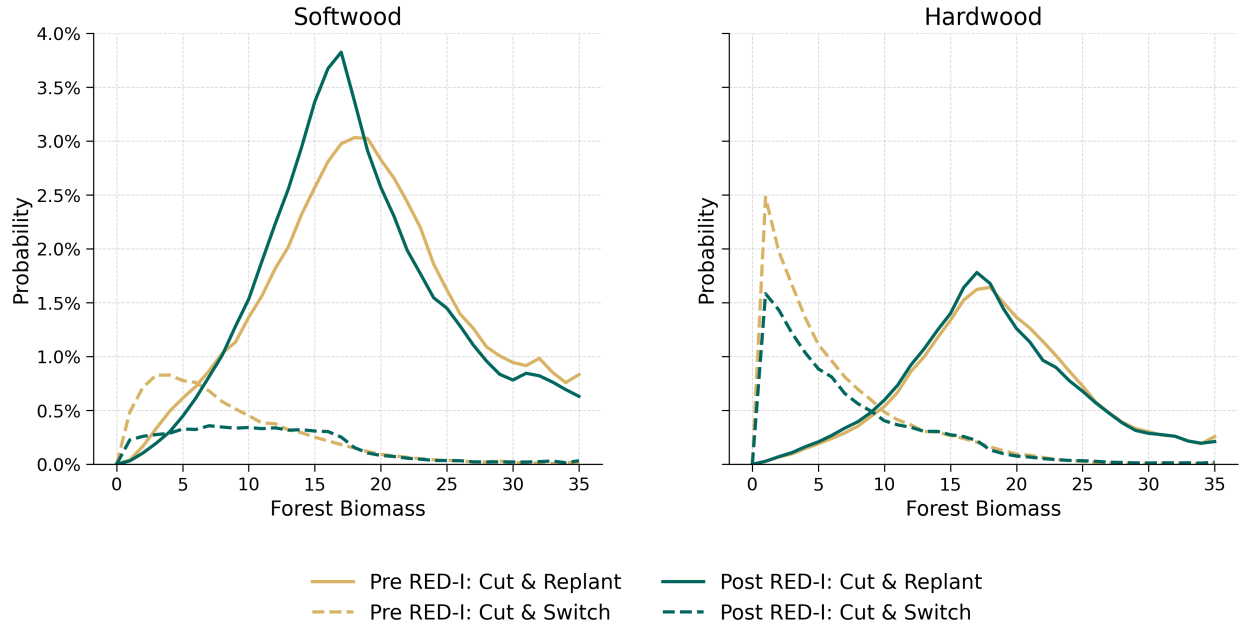
²¹Urban areas as of 2000 are excluded due to known LCMS misclassifications when urban canopy cover increases.

Table 1: Land Use Transitions

Land Use	Transition Matrix (2000–2023)		Land Use Shares	
	Forest	Non-Forest	2000	2023
Forest	95.7%	4.3%	77.5%	76.2%
Non-Forest	9.0%	91.0%	22.5%	23.8%

low biomass levels. Comparing the pre- and post-RED-I periods reveals two notable shifts. First, the probability of harvest and replant increased for lower biomass levels, consistent with stronger pulpwood demand from pellet mills. Second, the probability of harvests leading to conversion to non-forest uses declines for both forest types, with the relative decline larger for softwoods. While correlative, these shifts are consistent with stronger pulpwood demand changing harvest and replanting incentives in the post-RED-I period.

Figure 5: Annual Harvest Rates



Note: Cut and replant refers to events where the forest cover is lost, and the landuse remains forested, while cut and switch refers to events where the forest cover is lost, and the landuse switches to nonforest.

Product level prices come from Forest2Market (F2M) for pulpwood and sawtimber, separately for softwoods and hardwoods, across 33 wood-purchasing markets from 2001–2023.²² Each plot is assigned the corresponding market price for its forest type. Importantly, prices

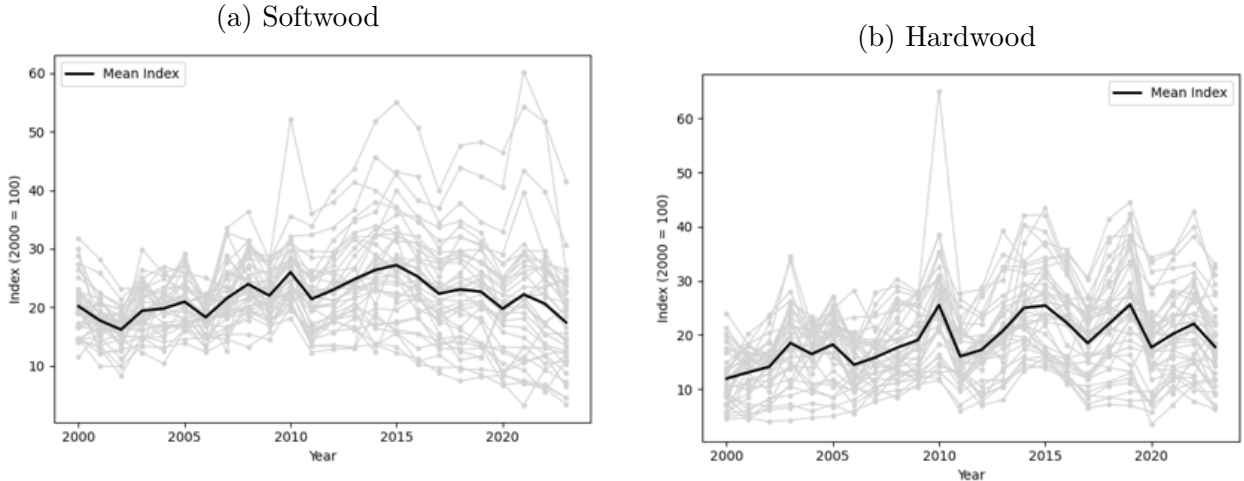
²²F2M markets are defined from transaction-level data between landowners and mills; see Appendix A for market boundaries.

are not for biomass, but are for the saw and pulp portions of the biomass on each plot. To align the biomass data with prices, I estimate the share of biomass which is saw, pulp, and residue as a function of the current biomass level for each wood type using the USFS Forest Inventory Analysis (FIA) ground-truth dataset. This provides the following set of estimated functions, denoted $\hat{\alpha}^{j,w}(b)$ where b is plot-level biomass of wood type, w , and the alpha function estimates the share of biomass that is of type j : saw, pulp, or residues. Using these estimated functions, I can then specify the relevant price index for a unit of biomass, which for a given forest type, w , is:

$$p^b = p^s \hat{\alpha}^s(b) + p^p \hat{\alpha}^p(b),$$

where p^s and p^p are the prices from F2M for the saw and pulp portions of the biomass, respectively.²³ Figure 6 shows pulpwood prices for both wood types.²⁴ Prices exhibit no structural break or persistent mean shift around RED-I, indicating limited price pass-through of European pellet-mill demand to local timber markets.

Figure 6: Pulpwood Prices, U.S. South Wood Markets



Note: All prices are displayed as indices to comply with provider restrictions. The mean market price of softwood sawtimber in the year 2000 is used as the index baseline, and all other data points are normalized relative to this value. Grey lines show individual market-level data.

Mill locations, ownership, openings, closures, type, and wood type for feedstock comes from the Forisk Mill Capacity database, supplemented with USFS and Southern Environmental Law Center records to extend coverage back to 2000.²⁵ To utilize this data, I calculate the

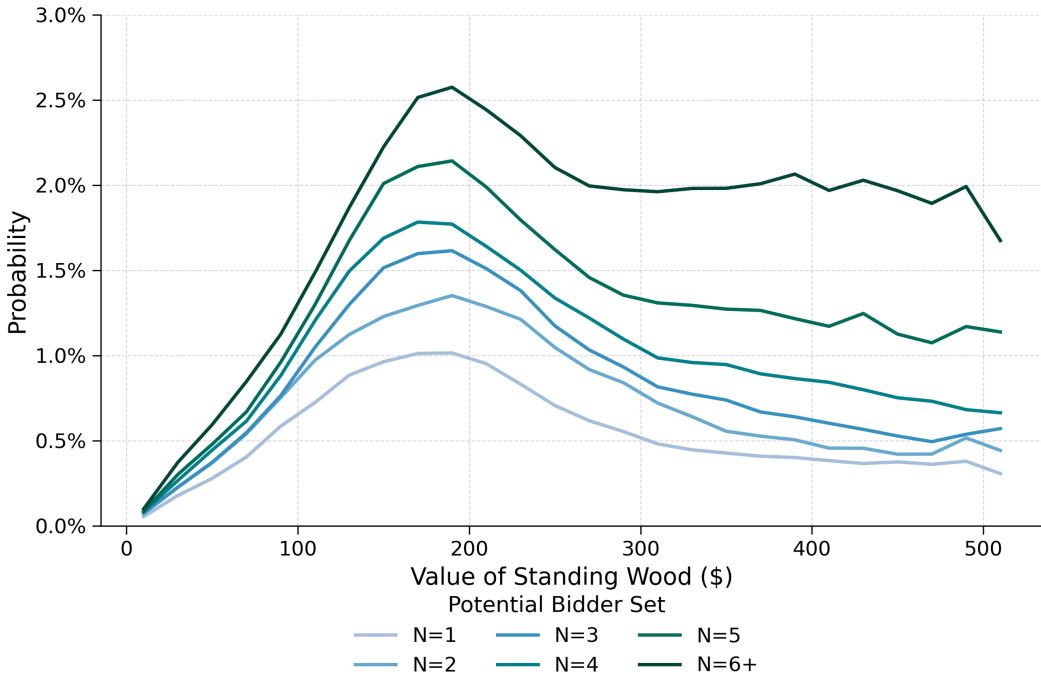
²³Estimation details and a description of USFS FIA data are provided in Appendix A.

²⁴Sawlog prices are presented in Appendix A.

²⁵See Appendix A for data assembly details.

potential bidder set for a given sale for each plot of land, denoted as N^w . The potential bidder set depends on the feedstock wood type mills purchase as landowners can only sell to mills who accept the matching type. For each plot, I calculate the potential bidder set N^w , which measures the number of distinct mill owners within 50 miles for softwood and 75 miles for hardwood plots.²⁶ Figure 7 shows that, holding wood value constant, harvest probability rises monotonically with the potential bidder set. This strong spatial correlation between market concentration and harvesting behavior provides descriptive evidence that local market structure may affect landowner decisions. This in turn may serve as a potential mechanism for policy transmission beyond price pass-through which appears limited in the data.

Figure 7: Annual Harvest Rate by Land Value and Potential Bidder Set



6. Model

The unit of analysis is a field of land indexed by i , which is managed by a profit-maximizing landowner. Each field is located in a submarket, denoted by m . In each year, t , landowners make a decision regarding land use for the next period. This decision is denoted by d_{it} . If the field is not forested, $d_{it} \in \{plant, out\}$, that is, they can plant trees or continue to choose the outside option.²⁷ For landowners with forested fields, $d_{it} \in \{wait, cut\}$, that is, they can

²⁶Transaction evidence shows typical haul distances of ≤ 55 miles for softwoods and ≤ 75 miles for hardwoods (Gibeault and Coutu, 2015).

²⁷The outside option can be thought of as either agricultural or development uses.

let the current forest grow and wait until the next period, or clear-cut all standing biomass.

I denote the state of a field's land use as $b_{it} \in \{0, 1, 2, \dots, \bar{B}\}$. If $b_{it} = 0$, the field is not forested, while for $b_{it} > 0$, the field is forested and b_{it} denotes the tons of aboveground biomass. I denote the exogenous state vector $\omega_{it} \in \Omega$, with information on the prices, mills, forest type, and cost shifters. All land is assigned a forest type, w , which denotes the current forest wood type if forested, and potential forest wood type if not forested. Finally, there is a state variable $\varepsilon_{it} \in \mathbb{R}^4$, which landowners observe but not the econometrician.

Growth in biomass on the field left to wait until next period follows a Markov chain with a $\bar{B} \times \bar{B}$ transition probability matrix F_w^b , which differs for each forest type, w . In other words, for a given plot of land, beliefs over future biomass are given by Markov transition probabilities:

$$F_{jk}^b = \Pr(b_{i,t+1}^w = k | b_{it}^w = j)$$

which is the same for $d \in \{plant, wait\}$, and is degenerate for each $d \in \{out, cut\}$ as $b_{it+1} = 0$ for these choices, regardless of the initial biomass level.

The number of potential mill buyers, N_{imt} , evolves according to a Markov transition matrix $F_{m,w}^N$ that varies by sub market m and wood type w . Similarly, the vector of wood prices by grade, g , P_{mt}^g , follows a grade-wood-type specific transition matrix F_w^{Pg} . Together, these processes characterize how both biological and market conditions evolve over time, shaping the landowner's dynamic optimization problem.

The flow payoff for land use decision d , is given by:

$$\Pi(d, s_{it}; \theta) = \pi(d, b_{it}, w_{it}; \theta) + \epsilon_{it}(d)$$

where $\pi(d, b_{it}, w_{it}; \theta)$ is a function that depends only on observed state variables and on a vector of parameters to be estimated, θ . Further, for each choice of d_{it} , there is a different unobserved state ϵ_{it} that represents a different unobserved state for each choice.

For fields not currently forested, where $b_{it} = 0$, the observed flow payoff $\pi(\cdot; \theta)$ is:

$$\pi(d, 0, \omega_{it}; \theta) = \begin{cases} \theta r_i + \theta^S 1(b_{i,t-1} > 0) & \text{if } d = \text{out} \\ \theta^P 1(b_{i,t-1} = 0) + \theta^R 1(b_{i,t-1} > 0) & \text{if } d = \text{plant} \end{cases}$$

The return index, r_i captures the payoff from non-forest uses. It is constructed using pasture suitability, and proximity to urban centers. I defer the discussion about the functional specification to the next section on estimation. Note that a field can have 0 biomass for two reasons: land use was previously non-forest, or land use was previously forest and was just

clearcut. If a field was previously non-forest $b_{it-1} = 0$, and remains non-forest, $d_{it} = out$, then $b_{it-1} = b_{it} = b_{it+1} = 0$ and the payoff is equal to the return index for the outside option. Similarly, when previously forested fields, $b_{it-1} > 0$, choose to transition to non-forest, $d_{it} = out$, then $b_{it} = b_{it+1} = 0$. In this case, landowners pay a fixed switching cost θ^S and earn the payoff from non-forest uses. When non-forest landowners plant trees on their field, i.e. $d_{it} = plant$, landowners pay a fixed tree planting cost. Planting costs θ^P or θ^R depend on previous land use.

For forested fields, where $b_{it} > 0$, the flow payoff $\pi(\cdot; \theta)$ is:

$$\pi(d, b_{it}, \omega_{it}; \theta) = \begin{cases} b_{it}(\theta X_i) + \theta_b b_{it} & \text{if } d = wait \\ b_{it}(\theta_r p_{it}^b(b_{it}) - \theta Z_i - g(N_{it}, \theta)) & \text{if } d = cut \end{cases}$$

If landowners chose to keep their forest until the next period, $d_{it} = wait$, then forests grow and the decision repeats next period. When choosing to wait, landowners pay variable maintenance costs θX_i . Here X_i is a vector of observable forest maintenance cost shifters, namely fire and insect/disease risk. Landowners may also have private costs or benefits directly associated with forest density, which are captured by θ_b . This value captures the net of private maintenance costs of biomass and private benefits from forest density (ex. aesthetic, bequest, hunting) and any internalized portion of the public value of biomass via government policies. If landowners chose to clearcut, $d_{it} = cut$, all biomass is removed and $b_{it+1} = 0$. A clearcut earns a payoff equal to the market stumpage price index for field i 's wood type, $p_{it}^b(b_{it})$ at the time of harvest.

Further, profits earned by a landowner are shifted with field-level harvest cost-shifters contained in Z_i , such as the slope of the land. Finally, profits are allowed to shift based on the potential bidder set, N_{it} , where higher values of N_{it} are expected to lead to higher profits. I approximate the markdown function with the following nonlinear form: $g(N_{it}, \theta) = \sum_{k=1}^{\bar{N}-1} \theta_k \mathbf{1}\{N_{int} = k\}$, where \bar{N} is described in the previous section. It is important to note that the choice to clearcut biomass, $d_{it} = cut$, is a renewal decision, resetting b_{it+1} to 0, and the landowner's choice set to $\{out, plant\}$.

Assumption 1. The unobserved state variables, $\epsilon_{it}(d)$, are independently and identically distributed over fields and time.

Assumption 2. The evolution of the exogenous state variables ω is not affected by landowner

decisions and ϵ , i.e.,

$$F_{\omega_{it+1}|d_{it}, \omega_{it}, \epsilon_{it}} = F_{\omega_{it+1}|\omega_{it}}.$$

Assumption 1 is standard in the dynamic discrete choice literature. Assumption 2 embeds several important underlying features. First, it implies that landowners are price takers, a reasonable assumption as many landowners own forest land. Second, landowner decisions don't alter expectations about future market structure. Third, it implies that choice-specific unobservables, ϵ do not change expectations about the evolution of ω . Finally, assumption 2 makes it clear that random shocks do not systematically influence biomass accumulation, the potential bidder set, or prices, and affect decisions like random noise.

I assume landowners discount future cash flows using a fixed discount rate $\beta < 1$. Landowners choose d_{it} every period conditional on $(b_{it}, \omega_{it}, \epsilon_{it})$ in order to maximize the sum of future discounted flow payoffs:

$$\max_{d_{it}} \mathbb{E} \left[\sum_{j=0}^{\infty} \beta^j \Pi(d_{i,t+j}, b_{i,t+j}, \omega_{i,t+j}, \epsilon_{i,t+j}; \theta) \middle| d_{it}, b_{it}, \omega_{it}, \epsilon_{it} \right].$$

I now rewrite the dynamic optimization problem faced by landowners as a recursive Bellman equation. When $b_{it} = 0$, which are all non-forested fields, the landowner can choose the outside option or to plant trees. In this case, the value function is:

$$V_\theta(0, \omega_{it}, \epsilon_{it}) = \max \left\{ \begin{aligned} & \pi(\text{out}, 0, \omega_{it}; \theta) + \epsilon_{it}(\text{out}) + \beta \mathbb{E} [V_\theta(0, \omega_{i,t+1}, \epsilon_{i,t+1}) | \omega_{it}], \\ & \pi(\text{plant}, 0, \omega_{it}; \theta) + \epsilon_{it}(\text{plant}) + \beta \mathbb{E} [V_\theta(b_{i,t+1}, \omega_{i,t+1}, \epsilon_{i,t+1}) | b_{it}, \omega_{it}] \end{aligned} \right\}.$$

When $1 \leq b_{it} \leq \bar{B}$, which are all forested fields, landowners can keep the forest or cut all the biomass. In this case, the value function is:

$$V_\theta(b_{it}, \omega_{it}, \epsilon_{it}) = \max \left\{ \begin{aligned} & \pi(\text{wait}, b_{it}, \omega_{it}; \theta) + \epsilon_{it}(\text{wait}) + \beta \mathbb{E} [V_\theta(\min(b_{i,t+1}, \bar{B}), \omega_{i,t+1}, \epsilon_{i,t+1}) | b_{it}, \omega_{it}], \\ & \pi(\text{cut}, b_{it}, \omega_{it}; \theta) + \epsilon_{it}(\text{cut}) + \beta \mathbb{E} [V_\theta(0, \omega_{i,t+1}, \epsilon_{i,t+1}) | \omega_{it}] \end{aligned} \right\}.$$

Assumptions 1 and 2 imply that expected continuation values do not depend on the present unobserved state ϵ_{it} . Further, Assumption 2, ensures that current choices do not alter the distribution of ω_{it+1} conditional on ω_{it} . Now let $\nu_\theta(d_{it}, b_{it}, \epsilon_{it})$ be the deterministic component

of each choice's value, that is,

$$\nu_\theta(d_{it}, b_{it}, \epsilon_{it}) = \pi(d_{it}, b_{it}, \omega_{it}; \theta) + \beta \mathbb{E} \left[V_\theta(\min(b_{it+1}(d_{it}, b_{it}), \bar{B}), \omega_{it+1}, \epsilon_{it+1}) \mid b_{it}, \omega_{it} \right]$$

where $(b_{it+1}(d_{it}, b_{it}))$ denotes the expected biomass next period given decisions and current biomass. The optimal choice, or policy function, is given by:

$$d^*(b_{it}, \omega_{it}, \epsilon_{it}) = \arg \max_d [v_\theta(d, b_{it}, \omega_{it}) + \epsilon_{it}(d)].$$

Since ϵ_{it} is unobserved to the econometrician, given observed state variables and parameters θ , we cannot observe the optimal choice. Instead, a conditional choice probability (CCP) can be constructed given the unobserved state distribution:

$$\Pr(d \mid b_{it}, \omega_{it}; \theta) = \int 1 \{ v_\theta(d, b_{it}, \omega_{it}) + \epsilon_{it}(d) \geq v_\theta(d', b_{it}, \omega_{it}) + \epsilon_{it}(d') \text{ for all } d' \} dG(\epsilon_{it}).$$

Assumption 3. $\epsilon_{it}(d)$ is independently and identically distributed across choice alternatives with type 1 extreme value distribution.

Assumption 3 implies the CCP has the usual logit form:

$$\Pr(d \mid b_{it}, \omega_{it}; \theta) = \frac{v_\theta(d, b_{it}, \omega_{it})}{\sum_{d'} v_\theta(d', b_{it}, \omega_{it})}.$$

This CCP is then used in the likelihood approach, described in the next section, that I use to estimate the model's vector of parameters θ .

7. Estimation

For estimation, I first sample from the full dataset along an evenly spaced 600-meter grid, yielding an estimation dataset of just over 5 million plots of land. I estimate the parameters in the model by Maximum Likelihood on data after RED-I to best reflect conditions in the post-policy period. The goal of estimation is to obtain the vector θ from observed states $\{b_{it}, \omega_{it}\}$ and decisions $\{d_{it}\}$. Assumption 2 implies that the evolution of the exogenous state does not depend on current endogenous states of landowner decisions. Therefore, I can write the conditional log likelihood function as:

$$L(\theta; (d_{it}, \omega_{it}, b_{it})) = \sum_t \sum_i \log f(\omega_{it} \mid \omega_{it-1}; \theta) + \sum_i \log (\Pr(d_i \mid \omega_i, b_i; \theta))$$

where I omit the subscript t to denote the whole vector of decisions and states.

In the set of exogenous state variables, ω_{it} , there are four variables that change over time for a given landowner ($p_{imt}^S, p_{imt}^P, b_{it}, N_{imt}$). For estimation purposes, I assume prices follow an AR(1) process, with market fixed effects.²⁸:

$$\begin{bmatrix} p_{mt}^S \\ p_{mt}^P \end{bmatrix} = \begin{bmatrix} k_m^S \\ k_m^P \end{bmatrix} + \begin{bmatrix} \lambda_S & 0 \\ 0 & \lambda_P \end{bmatrix} \begin{bmatrix} p_{mt-1}^S \\ p_{mt-1}^P \end{bmatrix} + \eta_{mt}, \quad (10)$$

where

$$\eta_{imt} \sim N \left(0, \begin{bmatrix} \sigma_S^2 & 0 \\ 0 & \sigma_P^2 \end{bmatrix} \right).$$

I then use the Tauchen (1986) discretization procedure with seven bins per market to convert the estimated AR(1) process into a discrete Markov process that can enter the computation of the CCP's in the second term of the likelihood function. As first-step estimates of the transition functions are of no direct interest by themselves, I report these results in Appendix B. Importantly, the AR(1) results show no violation of the required stationarity assumption.

Before estimating the remaining transition processes, I discretize the state space. The upper bound for biomass, \bar{B} , is set to 36, matching the typical maximum level of observed biomass in the data. The upper bound for the potential bidder set, \bar{N} , is set to 6, as few plots face more than six potential buyers. The remaining data discretization steps are described in Appendix B. For biomass and the count of potential bidders I estimate the empirical Markov transition process directly from the observed data. For biomass, I estimate the transition process separately for each wood type. The implied biomass dynamics from these transition functions are reported in Appendix B, which illustrate the expected growth trajectories implied by the estimated Markov processes. For the potential bidder set an empirical Markov transition process is estimated separately for each wood type, within each market. These discrete transition processes are then held fixed as the second term in the likelihood function is maximized with respect to the payoff parameters. To estimate payoff parameters, I use Aguirregabiria and Mira (2007)'s Nested Pseudo Likelihood (NPL) method.

7.1. Estimation Results

Table 2 below shows the results from the NPL estimation of the payoff parameters.

²⁸The VAR(1) specification is not used as cross-price correlations are rejected in the data for both wood types. Due to the presence of market fixed effects, the AR(1) processes are estimated via the Arellano–Bond system GMM estimator (Blundell and Bond, 1998).

Table 2: Payoff & Fixed Cost Parameter Estimates

	Out	Plant	
		θ^P	θ^R
$\theta_{\text{Pasture SI}}$	0.0221*** (0.0016)		-3.5639*** (0.0356)
$\theta_{\text{Accessibility}}$	-0.0618*** (0.0016)		-4.0733*** (0.0056)
θ^S	-7.0154*** (0.0334)		
	Wait	Cut	
θ_{AGB}	-0.0084*** (0.0001)	$\theta_{\text{AGB} \times \text{Price}}$	0.0115*** (0.0001)
$\theta_{\text{AGB} \times \text{Insect}}$	-0.0006*** (0.0000)	$\theta_{\text{AGB} \times \text{Slope}}$	-0.0032*** (0.0000)
		θ_{Residue}	-0.5603*** (0.0057)
		$\theta_{\text{AGB} \times N=1}$	-0.0469*** (0.0005)
		$\theta_{\text{AGB} \times N=2}$	-0.0321*** (0.0004)
		$\theta_{\text{AGB} \times N=3}$	-0.0239*** (0.0004)
		$\theta_{\text{AGB} \times N=4}$	-0.0174*** (0.0004)
		$\theta_{\text{AGB} \times N=5}$	-0.0092*** (0.0004)

Note: Standard errors in parentheses. *** $p < 0.01$, ** $p < 0.05$, * $p < 0.1$.

Both pasture suitability and accessibility to urban centres play a significant role in determining the value of the outside option. First, the estimate for pasture implies that the most suitable plots for pasture are 54% more valuable than the worst. Next, estimates for accessibility show that plots closest to urban cores have an annualized value 24 times higher than those in the hinterlands. This substantial variation in the value of the outside option allows landowner incentives to vary widely across space.

Since conversion from forest to non-forest land uses require substantial clearing operations (e.g., stump removal), the fixed costs of exiting forestry should exceed tree planting costs, a pattern corroborated by the results. On the other hand, the results show that the costs of converting marginal farmland to forest is lower than for replanting trees post-harvest. This could be due to lower land clearing and preparation fees, but is likely also driven by the presence of subsidies provided to forest land use conversion, such as the USDA Conservation Reserve Program.

How landowners value above-ground biomass is not a priori obvious, as it reflects the net of private benefits (e.g., amenity, recreational value, etc.) and internalized public benefits (e.g. value of carbon) and variable maintenance costs. The results indicate that private costs are larger than benefits, implying that landowners pay significant maintenance costs to upkeep current forests. Forest maintenance costs are also found to shift significantly with insect risk. The results imply that insect risk increases variable upkeep costs from \$0 to \$1.5 per ton of on-site biomass.

The payoffs for landowners cutting their forest imply that higher sloped plots face higher

harvesting costs, as expected. Further, there are large estimated disposal costs for residues, accounting for 15% of replanting costs. Residue disposal costs provides another subtle reason why harvest rates for hardwoods are lower as they have a higher share of residues at all levels of biomass. For the modal harvest volume, the residue removal costs on hardwood plots are roughly 30% higher than for softwood plots. Finally, the impact of market power is significant and is monotonically decreasing as the number of potential bidders increases. The estimates imply that monopsonists lower the average sale price by 40%, while going from 6+ bidder to 5 lowers the average sale price by 8%. This is similar to the change in prices observed in the timber auction literature from changing competition levels (Baldwin et al. (1997), Préget and Waelbroeck (2012)).²⁹

8. Counterfactual Simulations

The purpose of the counterfactual simulations is to quantify how much of the observed forest dynamics (i.e., harvesting, planting, carbon flux) can be attributed to the pellet mills that entered due to RED-I. To do so, I use the estimated transition and payoff parameters to simulate the evolution of the forest under alternative policy scenarios. The simulations begin from the empirical distribution of 2009 observations, which defines the initial mass of plots from the full dataset in each discrete state of the model's state space.

First, I simulate the business-as-usual case which reflects the actual data conditions used in estimation where pellet mills have entered and begun production. Then, I develop a counterfactual where for each landowner, I recalculate N_{imt} without pellet mills, which I denote as N'_{imt} . I then re-estimate the transition function for the potential bidder set with N'_{imt} to capture the evolution of mills that would have occurred had pellet mills not entered.

The central threat to the validity of this counterfactual is that pellet mills may have induced entry or exit of other mill types. In Appendix C, I estimate a staggered event-study at the market-level and show that there is no statistically significant effect on the number of non-pellet mills. When disaggregated by mill type, I find a marginally significant effect suggesting that pellet mills induced entry of hardwood sawmills. This would imply that this approach understates the change in competition, and the results presented below represent a lower bound on the effect of pellet mills.³⁰

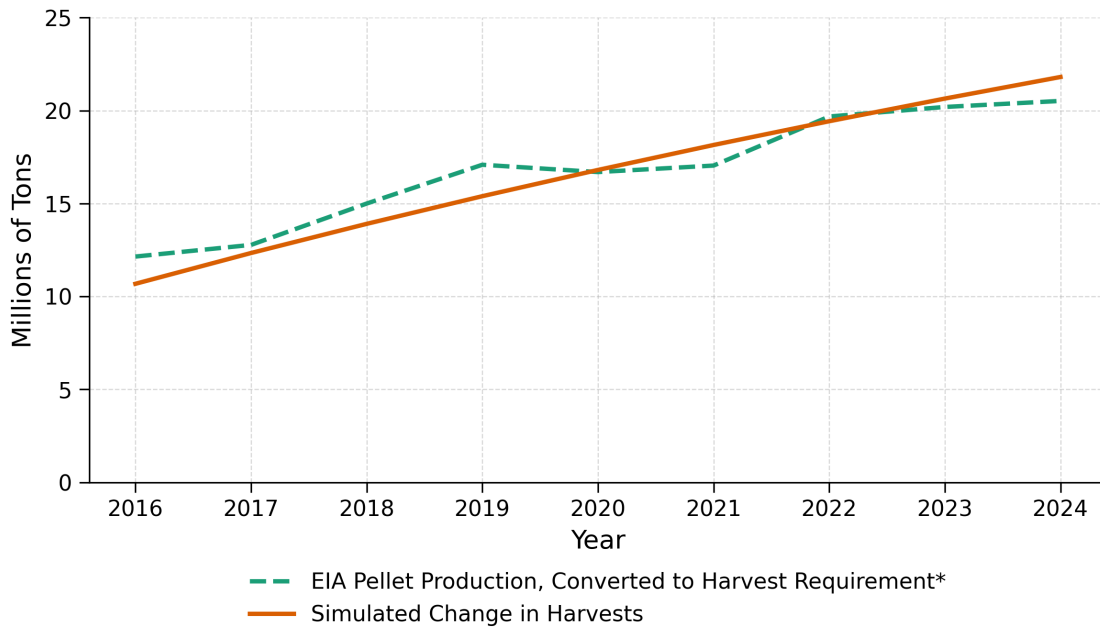
By comparing simulated harvested volumes with and without pellet mills, I obtain an

²⁹Distance to roads, elevation, fire risk, and cotton yields had an imprecise effect (not statistically different from zero) in earlier specifications and were removed for the sake of parsimony.

³⁰These results also confirm that, at the market level, pellet mills represent new potential bidders, as the total number of unique bidders increases by a similar magnitude to the number of pellet mills entering.

estimate of the incremental harvest attributable to RED-I. This can then be compared to pellet production by converting the U.S. EIA's reported industry output to expected harvest demand.³¹ Figure 8 shows that during the years in which EIA tracks pellet production, the model predicts harvest increases roughly equivalent to the harvest demand implied by pellet output. This suggests that pellet production has been supplied largely from new harvests rather than improved waste wood recovery. The estimated increase in this time period harvests represents a 2% increase in harvest volume across the entire study region, which while measured at a broader scale, is consistent with other studies estimating the impact of pellet mills on harvesting rates. Specifically, Williams and Xi (2021) finds a 16% increase harvested area within 60 miles of a set of selected pellet mills, while Parajuli et al. (2024) find a persistent, though statistically insignificant, 10-15% increase in market-level pulpwood harvests in markets where pellet mills enter.

Figure 8: Pellet Production vs. Simulated Change in Harvests



Note: EIA Form 63C provides U.S. South wide pellet production. I convert this to required tons of forest harvest by multiplying each output ton by the industry standard 2.2 to convert to green-weight input requirement.

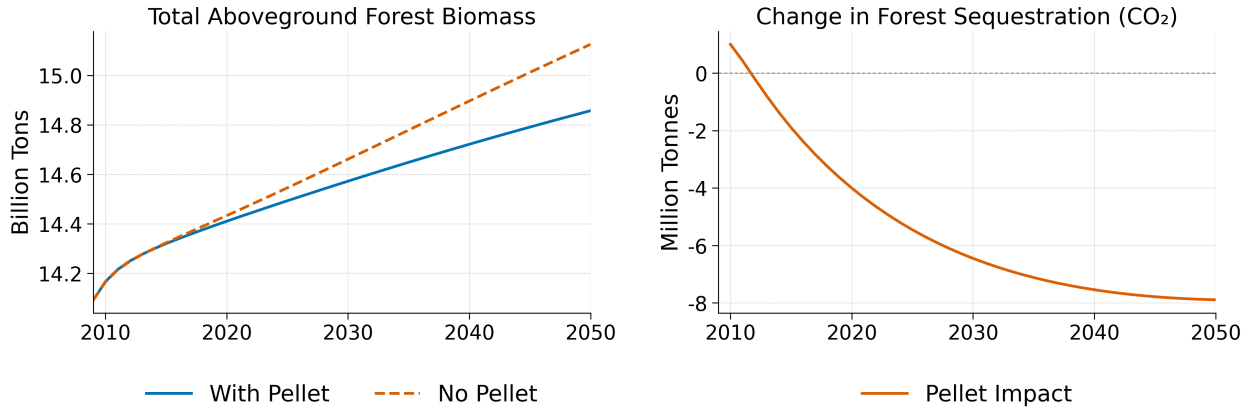
Since the increase in harvested biomass suggests a market response closer to the 100% new harvest scenario discussed in Section 4, the carbon implications of the policy now depend on whether the forest carbon sink increases. The left panel of Figure 9 shows simulated forest biomass with and without pellet mills, while the right panel reports the net change in annual

³¹A common assumption is that one ton of pellets requires 2.2 tons of harvested biomass at the mill gate, though this ratio can rise in high-moisture years or with shifts in species mix.

CO_2 sequestration rate due to pellet mills. Initially, relative to the no pellet counterfactual, landowners delayed harvests in anticipation of future pellet entry and lower markdowns. This results in temporarily higher forest biomass with pellet mills in the first three years. However, by year 4, forest biomass falls below the no pellet counterfactual. By 2050, the counterfactual world without pellet mills would have accumulated 1.8% more forest biomass.

In terms of carbon flux, this dynamic produces an initial increase in carbon sequestration due to pellet mills for the first two years, followed by a long decline over the following decades. In 2024, the model predicts that the forest removed ≈ 5 million tonnes less CO_2 from the atmosphere compared to the counterfactual, equivalent to about 1.4% of total U.K. emissions. If valued on the EU ETS as energy-related carbon emissions, this lost sequestration would correspond to roughly \$1.8 billion at 2024 market prices. The social cost of the total loss in forest carbon flux is \$53 billion (2020 USD) through 2050.³² Longer run projections in Appendix D show the simulated reduction in the carbon land sink persists well beyond 2050, lasting for centuries. Framed alternatively, wood bioenergy policies permanently reduce the carbon land sink, L_t , defined in Section 4. That is what looked bad at the smokestack, is now worse when we analyze the forest account in detail.

Figure 9: Forest Biomass & Carbon Flux



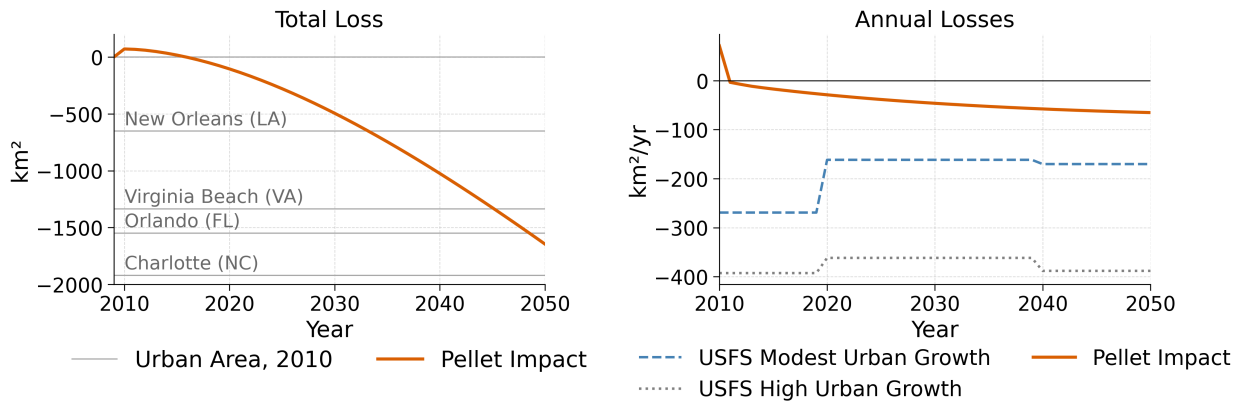
This result may appear counterintuitive as higher effective prices paid to landowners lead to a lower long-run supply of forest biomass. However, this outcome is driven by imperfect post-harvest replanting which leads to increased forest losses over time. In the absence of pellet production, the U.S. Forest Service (USFS) projections show that total forest area in the U.S. South is expected to decline through 2050 due to suburban encroachment from

³²The social cost is valued using the approach and methods from U.S. Environmental Protection Agency (2023).

urban growth. The model's results show with pellet mills landowners increase the rate of forest conversion relative to the no pellet counterfactual.

The left panel of Figure 10 shows the additional km^2 of forest loss with pellets compared to the counterfactual. By 2050, the model predicts more than $1500 km^2$ of additional cumulative forest loss, larger than the entire urban area of Orlando in 2010. The right panel the model's simulated annual rate of forest loss with the USFS's projected losses from urbanization under two alternative urban growth scenarios. Two patterns emerge. First, the rate of forest loss due to pellet mills continues to rise through 2050.³³ Second, by 2050, the presence of pellet mills increases the projected rate of forest loss by 16% – 38%, depending on the urban growth scenario. This loss in forest land represents the extensive margin through which long-run biomass declines. On the intensive margin, higher harvest rates from a shrinking forest base lowers the average biomass per field compounding the total loss of forest carbon over time.

Figure 10: Forest Loss from Wood Bioenergy



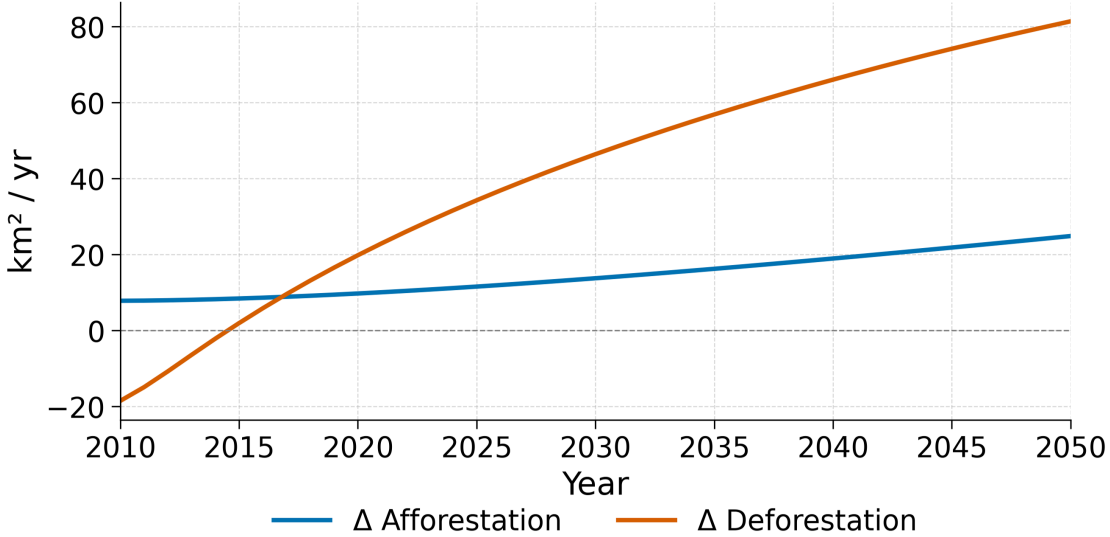
Even though forest area and biomass both decline due to to pellet mill entry, the model predicts changes in landowner behavior consistent with theoretical expectations. Figure 11 shows that afforestation increases in response due to reduced markdowns, as expected. However, as post-harvest replanting remains incomplete there more land use conversion due to increased harvesting.³⁴ As a result, the gains in forest area from higher planting and replanting are outweighed by the forest area lost from additional harvests that are not replanted. The model shows that the increase in deforestation, driven by imperfect replanting, is larger than the additional afforestation and stays larger over the planning horizon. Consequently, despite more frequent planting and replanting, forest area continues

³³In Appendix D's long-run simulation, losses do not fully stabilize and over $12,000 km^2$ is projected to be lost by 2250.

³⁴On average, only $\approx 82\%$ of harvested plots are replanted

to shrink, leading to lower biomass accumulation over time.

Figure 11: Afforestation vs. Deforestation



In Table 3, I decompose the cumulative change in forest carbon through 2050 by wood type, accessibility, and pasture suitability to identify where bioenergy-driven land-use change most affects carbon stocks. The results reveal important heterogeneity in the results across forest types and site characteristics. First, losses are dominated by hardwood forests, which together account for 84% of the lost forest carbon, reflecting both higher baseline conversion probabilities and slower regrowth rates. Further, across forest types, forest carbon losses are concentrated in high- and mid-accessibility zones, where forests face greater development and conversion pressure. In contrast, softwood forests in low-accessibility, low-suitability areas exhibit forest carbon gains, reflecting both lower land conversion risk and faster regrowth rates. This spatial heterogeneity demonstrates that the overall carbon impact of wood-bioenergy policy depends on the types of forests harvested and their surrounding land-use incentives.

9. Conclusion

This paper develops a dynamic structural model of forest harvesting and land use to quantify the long-run effects of wood bioenergy subsidies on forest dynamics and carbon sequestration. The model links landowner decisions to local buyer concentration, capturing how pellet mill entry from RED-I changed harvesting intensity, forest area, and forest carbon flux over time. The results indicate that the marginal unit of wood supplied by U.S. South wood markets to meet European bioenergy demand has been sourced primarily from new harvests rather than waste wood, creating a carbon debt that can only be repaid through

Table 3: Decomposition of Cumulative Change in Forest Carbon

Wood Type	Accessibility	Pasture Suitability	ΔCO_2 (MMT)	
Hardwood	High	High	-27.6	
		Mid	-48.3	
		Low	-16.5	
	Mid	High	-24.1	
		Mid	-46.5	
		Low	-14.5	
	Low	High	-12.0	
		Mid	-8.7	
		Low	19.3	
Hardwood Subtotal			-178.9	
Softwood	High	High	-30.0	
		Mid	-22.7	
		Low	-13.1	
	Mid	High	-16.9	
		Mid	-15.0	
		Low	1.9	
	Low	High	15.0	
		Mid	16.5	
		Low	28.1	
Softwood Subtotal			-36.2	
Total			-215.1	

subsequent forest regrowth. Although landowners received higher effective prices from pellet mill entry, due to lower markdowns, the increase in tree planting is insufficient to offset the forest loss arising from imperfect post-harvest replanting. As a result, the model predicts a persistent decline in forest biomass and carbon sequestration, implying that bioenergy policies reduced the long-run carbon sink potential of U.S. South forests.

These findings challenge the implicit premise underlying wood bioenergy subsidies: that future sequestration will offset combustion emissions and the lost sequestration from leaving trees in the ground. This underscores the importance of designing policy frameworks that account for land-use switching, imperfect replanting, and substitution effects across mills. Analyses that treat markets as static or analyze short-run equilibria miss the feedback between prices, harvesting, and replanting that determine long-run forest carbon outcomes. By explicitly modeling imperfect replanting and endogenous land-use transitions, this paper shows that policies which appear carbon-neutral can, over time, generate cumulative carbon losses over time. Accounting for these dynamic adjustments is essential for accurately assessing the true climate impacts of renewable energy incentives.

A key implication is that current international carbon-accounting frameworks overstate the climate benefits of wood bioenergy. Under current conventions, emissions from bioenergy combustion are counted as zero in the energy sector and are assumed to balance over time in the forest sector. Yet these accounts lack the spatial and temporal resolution to identify whether forest regrowth actually repays any incurred carbon debt. As a result, policies can appear to offset in official inventories even when they reduce the long-run forest carbon sink. Incorporating market-based estimates of the impact on forest carbon flux, such as those developed in this paper, would substantially improve the accuracy of global carbon accounting for wood bioenergy. This problem would not be solved even if carbon-capture technology were added at the smokestack; the continued loss of forest carbon from new harvests and imperfect replanting would still yield net emissions. In short, the forest carbon losses dominate, meaning that current policies, even when coupled with carbon capture, cannot deliver genuine carbon benefits without changes in sourcing or replanting requirements.

The analysis also provides insights into how to improve the current policy regime to achieve real climate benefits. By decomposing the results across the spatial heterogeneity in the data, I show that carbon losses are concentrated in hardwood forests and in areas with high development pressure and agricultural value. In softwood forests with low development and agricultural value, the pattern reverses, with climate benefits emerging by 2050. This spatial heterogeneity suggests that the overall carbon effect of bioenergy policy depends on which forests the wood is sourced from. This suggests that existing policy frameworks such as the

EU Deforestation Regulation (EUDR) and the U.K.’s forthcoming Forest Risk Commodity Regulation should integrate spatial sourcing criteria. By incorporating spatial targeting, these deforestation laws could ensure that renewable energy policies deliver genuine climate benefits.

The framework developed here suggests a number of future research directions. Beyond bioenergy, the framework developed here offers a general tool for analyzing forest sector responses to policy shocks that alter the spatial and temporal distribution of wood demand. The same approach could be applied to assess the forest and carbon consequences of policies that increase harvesting pressure, such as bans or taxes on plastic packaging that raise paper demand, incentives for mass timber construction, or the expansion of carbon credit markets.

Additional extensions could enrich the modeling framework itself. Incorporating a dynamic model of mill entry would allow for a richer analysis of the impact of proposed sourcing restrictions on entry location and market structure. Embedding such a dynamic model within the dynamic landowner framework remains an empirical and theoretical challenge due to the presence of two-way expectations. It may also be possible to relax several assumptions in the model by incorporating additional data. For instance, parcel-level property ownership data would allow for a more natural modeling of aggregated harvest blocks and capture economies of scale in harvest choices. Future work could incorporate forest mortality due to natural disturbances to capture how the presence of standing dead and decomposing biomass affects the policy results. Finally, extending the model to include thinning harvests, in which only a portion of forest biomass is removed, would align the model more closely with forestry practices in the U.S. South. However, this would require maps of partial forest loss or other measures of forest degradation—an emerging field in remote sensing.

References

- Abt, K. L., Abt, R. C., Galik, C. S., and Skog, K. E. (2014). Effect of policies on pellet production and forests in the u.s. south. Technical report, USDA Forest Service, Southern Research Station.
- Aguilar, F. X., Sudekum, H., McGarvey, R., Knapp, B., Domke, G., and Brandeis, C. (2022). Impacts of the us southeast wood pellet industry on local forest carbon stocks. *Scientific Reports*, 12(19449).
- Aguirregabiria, V. and Mira, P. (2007). Sequential estimation of dynamic discrete games. *Econometrica*, 75(1):1–53.
- Araujo, R., Costa, F. J. M., and Sant’Anna, M. (2025). Efficient conservation of the brazilian amazon: Estimates from a dynamic model. *Review of Economic Studies*. Forthcoming.
- Athey, S. and Levin, J. (2001). Information and competition in u.s. forest service timber auctions. *Journal of Political Economy*, 109(2):375–417.
- Athey, S., Levin, J., and Seira, E. (2011). Comparing open and sealed bid auctions: Evidence from timber auctions. *Quarterly Journal of Economics*, 126(1):207–257.
- Baldwin, L. H., Marshall, R. C., and Richard, J.-F. (1997). Bidder collusion at forest service timber sales. *Journal of Political Economy*, 105(4):657–699.
- Barnett, K., Aplet, G. H., and Belote, R. T. (2023). Classifying, inventorying, and mapping mature and old-growth forests in the united states. *Frontiers in Forests and Global Change*, 5:1070372.
- Blundell, R. and Bond, S. (1998). Initial conditions and moment restrictions in dynamic panel data models. *Journal of Econometrics*, 87(1):115–143.
- Butler, B. J. and Wear, D. N. (2013). Forest ownership dynamics of Southern forests. Technical Report SRS-GTR-170, USDA Forest Service, Southern Research Station.
- Caputo, J. and Butler, B. (2025). National woodland owner survey dashboard (nwos-dash) version 1.0.
- Department for Energy Security and Net Zero (2025). Digest of United Kingdom energy statistics (DUKES): Annual data for 2024, chapter 6. Technical report, Department for Energy Security and Net Zero.

- Duden, A. S., Verweij, P. A., Faaij, A. P. C., Abt, R. C., Junginger, M., and van der Hilst, F. (2023). Spatially-explicit assessment of carbon stocks in the landscape in the southern us under different scenarios of industrial wood pellet demand. *Journal of Environmental Management*, 342:118148.
- European Commission (2021). Study on energy subsidies and other government interventions in the European Union. Technical report, Trinomics B.V.
- European Commission (2024). State of the energy union report 2024. Technical Report COM(2024) 404 final, European Commission.
- European Commission, Joint Research Centre (2024). Simulating future wood consumption and the impacts on Europe's forest sink to 2070. Technical Report EUR 31887 EN, European Commission, Joint Research Centre.
- FAO and IIASA (2007). Suitability of global land area for pasture (fggd), version 1.0. Food and Agriculture Organization of the United Nations (FAO), Rome, Italy.
- Faustmann, M. (1849). Calculation of the value of forest soil and uncut timber stocks for the world economy. *General Forestry and Hunting*, 25:441–455.
- Forest2Market (2015). Wood supply trends in the US South, 1995–2015. Technical report, Forest2Market, Inc.
- Gibeault, F. M. and Coutu, P. J. (2015). Wood supply chain component costs analysis: A comparison of Wisconsin and U.S. regional costs—2015 update. Technical report, Steigerwaldt Land Services, Inc. and Forest2Market, Inc.
- Grove, G., Conrad, J. L., Harris, T. G., and Dahlen, J. (2019). Consulting forester timber sale practices in the us south. *Forest Science*, 66(12):749–756.
- Guo, C. and Costello, C. (2013). The value of adaptation: Climate change and timberland management. *Journal of Environmental Economics and Management*, 65(3):452–468.
- Haile, P. A. (2001). Auctions with resale markets: An application to u.s. forest service timber sales. *American Economic Review*, 91(3):399–427.
- Hansen, M. C., Potapov, P. V., Moore, R., Hancher, M., Turubanova, and et al. (2013). High-resolution global maps of 21st-century forest cover change. *Science*, 342(6160):850–853.
- Hartman, R. S. (1976). The harvest decision when a standing forest has value. *Economic Inquiry*, 14(1):52–63.

- Hashida, Y. and Lewis, D. J. (2019). The intersection between climate adaptation, mitigation, and natural resources: An empirical analysis of forest management. *Journal of the Association of Environmental and Resource Economists*, 6(5):1069–1104.
- Howarth, R. W. (2024). The greenhouse gas footprint of liquefied natural gas (lng) exported from the united states. *Energy Science & Engineering*.
- Hsiao, A. (2025). Coordination and commitment in international climate action: Evidence from palm oil. *Stanford University Working Papers*. Working paper.
- Johnson, T. G., Bentley, J. W., and Howell, M. (2011). The South’s timber industry—an assessment of timber product output and use, 2009. Technical Report SRS-182, USDA Forest Service, Southern Research Station.
- Johnson, T. G. and Steppleton, C. D. (2002). Southern pulpwood production, 2000. Technical report, USDS Forest Service, Southern Research Station.
- Johnson, T. G. and Steppleton, C. D. (2011). Southern pulpwood production, 2009. Technical report, USDS Forest Service, Southern Research Station.
- Kennedy, R. E., Ohmann, J., Gregory, M., Roberts, H., Yang, Z., Bell, D. M., Kane, V., Hughes, M. J., Cohen, W. B., and Powell, S. (2018). An empirical, integrated forest biomass monitoring system. *Environmental Research Letters*, 13(2):025004.
- Krist, F. J. J., Ellenwood, J. R., Woods, M. E., McMahan, A. J., and et al. (2014). 2013–2027 national insect and disease forest risk assessment: Summary and data. Technical report, U.S. Department of Agriculture, Forest Service, Forest Health Technology Enterprise Team.
- Kuehn, Z. (2019). Estimating auctions with externalities: The case of u.s. forest service timber auctions. *Review of Economics and Statistics*, 101(5):791–807.
- Li, T. and Perrigne, I. (2003). Timber sale auctions with random reserve prices. *Review of Economics and Statistics*, 85(1):189–200.
- Parajuli, R., Brandeis, C., and Chizmar, S. (2024). Impacts of the european renewable energy policy on forest resource markets in the southern united states: A case of the wood pellet industry. *Resources, Conservation and Recycling*, 207:107692.
- Potapov, P., Tyukavina, A., Hansen, M. C., Pickens, and et al. (2022). Global trends of forest loss due to fire from 2001 to 2019. *Frontiers in Remote Sensing*, 3:825190. Section: Remote Sensing Time Series Analysis.

- Provencher, B. (1995a). An investigation of the harvest decision of timber firms in the south-east united states. *Journal of Environmental Economics and Management*, 29(3):321–338.
- Provencher, B. (1995b). Structural estimation of the stochastic dynamic decision problems of resource users: An application to the timber harvest decision. *Journal of Environmental Economics and Management*, 29(3):321–338.
- Préget, R. and Waelbroeck, P. (2012). What is the cost of low participation in french timber auctions? *Applied Economics*, 44(11):1337–1346.
- Rust, J. and Paarsch, H. J. (2020). Implementing faustmann–marshall–pressler at scale: Stochastic dynamic programing in space. In de Paula, , Tamer, E., and Voia, M.-C., editors, *The Econometrics of Networks*, volume 42 of *Advances in Econometrics*.
- Sackett, J. (2023). Southeast U.S. wood pellet plants database. Southern Environmental Law Center.
- Sant'Anna, M. (2024). How green is sugarcane ethanol? *Review of Economics and Statistics*, 106(1):202–216.
- Sass, E. M., Markowski-Lindsay, M., Butler, B. J., Caputo, J., Hartsell, A., Huff, E., and Robillard, A. (2021). Dynamics of large corporate forestland ownerships in the united states. *Journal of Forestry*, 119(4):363–375.
- Schelhas, J., Brandeis, T. J., and Rudel, T. K. (2021). Planted forests and natural regeneration in forest transitions: patterns and implications from the u.s. south. *Regional Environmental Change*, 21(2):42.
- Scott, J. H., Dillon, G. K., Jaffe, M. R., Vogler, and et al. (2024). Wildfire risk to communities: Spatial datasets of landscape-wide wildfire risk components for the united states (2nd edition).
- Scott, P. T. (2014). Dynamic discrete choice estimation of agricultural land use. *Toulouse School of Economics Working Papers*, 14-526.
- Smith, M., Elsaïd, S., Finesso, A., and Kiewiet de Jonge, T. (2022). Government subsidies for electricity generation and combined heat and power (chp) from solid biomass. Technical report, Trinomics B.V.
- Spelter, H. and Alderman, M. (2005). Profile 2005: Softwood sawmills in the united states and canada. Technical report, USDA Forest Service, Forest Products Laboratory.

- Spelter, H., McKeever, D., and Toth, D. (2009). Profile 2009: Softwood sawmills in the united states and canada. Technical report, USDA Forest Service, Forest Products Laboratory.
- Spelter, H. and McKeever, T. (1999). Profile 1999: Softwood sawmills in the united states and canada. Technical report, USDA Forest Service, Forest Products Laboratory.
- Tauchen, G. (1986). Finite state markov-chain approximations to univariate and vector autoregressions. *Economics Letters*, 20(2):177–181.
- Tran, H., Juno, E., and Arunachalam, S. (2023). Emissions of wood pelletization and bioenergy use in the united states. *Renewable Energy*, 219(Part 2):119536.
- UK National Audit Office (2025). The government's support for biomass. Technical report, National Audit Office.
- U.S. Environmental Protection Agency (2023). Report on the social cost of greenhouse gases: Estimates incorporating recent scientific advances. Technical report, U.S. Environmental Protection Agency, Washington, DC.
- U.S. Geological Survey (2019). 3d elevation program 1-meter resolution digital elevation model. U.S. Geological Survey Data Release.
- U.S. Geological Survey (2024). Protected areas database of the united states (pad-us) 4.0 raster analysis. U.S. Geological Survey Data Release.
- USDA Forest Service (2025). Usfs landscape change monitoring system (lcms), conterminous united states, version 2024-10.
- Wear, D. N. and Greis, J. G. (2013). The southern forest futures project: Technical report. General Technical Report SRS-GTR-178, USDA Forest Service, Southern Research Station.
- Weiss, D. J., Nelson, A., Gibson, H. S., and et al. (2018). A global map of travel time to cities to assess inequalities in accessibility in 2015. *Nature*, 553:333–336.
- Williams, C. A., Hasler, N., Gu, H., and Zhou, Y. (2020). Forest carbon stocks and fluxes from the nfcms, conterminous usa, 1990–2010 (version 2).
- Williams, C. A. and Xi, L. (2021). Forest clearing rates in the sourcing region for enviva pellet mills in virginia and north carolina, u.s.a. Technical report, Clark University.
- Wu, T., Lin Lawell, C. Y. C., Just, D. R., Zhao, J., Fei, Z., and Wei, Q. (2022). Optimal forest management for interdependent products: A nested dynamic bioeconomic model and application to bamboo. *AgEconSearch Working Paper*.

A. Data

In this section, I provide details on how the core datasets used in the paper are merged and aligned with one another. First, I describe how I temporally align the three separate panel datasets derived from remote sensing which measure the core decision and stock variables: land use, biomass, and forest loss. Subsequently, I detail the construction of the mill dataset, which combines mill capacity data from Forisk and the U.S. Forest Service (USFS) to create a time series of wood-receiving mills spanning from 2000 through 2023. I then describe how this mill dataset is used to calculate key market structure measures around individual plots. I continue by describing how the stumpage price dataset is mapped to individual plots. I then introduce the USFS FIA database and the estimation method used to convert biomass into sawtimber and pulpwood to align with the price data. Finally, I also discuss the creation of additional regressors used in the paper.

All datasets, except for mills, prices, and the FIA database are spatial raster files. These raster datasets are spatially merged on a common grid. The table below summarizes the data source for each variable used in the paper, along with its initial measurement scale. The final dataset consists of approximately 1.22 billion observed plots of land from 2001 to 2023. As described below, we restrict the data to remove pre-existing urban areas, water, and protected land to obtain 1.03 billion plots. Finally, to make the dataset computationally tractable for descriptive and econometric analysis, I sample it along an evenly spaced 600m grid, yielding a balanced panel of roughly 5.15 million plots over the study period.

Table A.1: Data Sources and Resolution

Variable Name	Data Source	Resolution
Land Use	USDA Forest Service (2025)	30 m
LCMS Forest Change	USDA Forest Service (2025)	30 m
GFW Forest Loss	Hansen et al. (2013)	30 m
Forest Loss due to Fire	Potapov et al. (2022)	30 m
Aboveground Biomass	Kennedy et al. (2018)	30 m
Protected Areas	U.S. Geological Survey (2024)	30 m
Forest Type in 2000	Williams et al. (2020)	30 m
Pasture Suitability	FAO and IIASA (2007)	10 km
Slope	U.S. Geological Survey (2019)	30 m
Fire Risk	Scott et al. (2024)	30 m
Insect Risk	Krist et al. (2014), Projected Loss Rate	250 m
Site Remoteness	Weiss et al. (2018)	1 km

A.1. Decision and Biomass Data Alignment

Due to differences in the underlying methods to create each remote sensing dataset, I first must ensure temporal consistency across land use, biomass, and forest loss measures. I first restrict the sample by removing protected areas, water, and pre-existing urban areas. I first address spurious transitions from urban to forest, commonly observed in remote sensing data due to urban tree growth but rarely supported by ground truth, by enforcing persistence of developed land use classes. I next simplify land use categories into forest and non-forest, where non-forest includes agriculture, pasture, urban, and bare land. I then remove transient transitions, forest to non-forest and back, that last two periods or fewer from the time series. These are mainly related to temporary transitions to bare land after harvesting or natural disturbances.

Next, I align the land use, forest loss, and biomass datasets to ensure temporal consistency across them, as each is derived from separate machine learning algorithms applied to Landsat imagery. We first align the land use measure and Global Forest Loss (GFW) loss dates. Due to differences in the time of year of the satellite images used in the machine learning algorithms underlying these datasets, land use transitions may occur early (i.e. in the year of harvest) when there is a forest loss event. For these cases, I set the land use transition to occur exactly one year following GFW-detected loss events. This ensures that losses occur on forested lands and transitions occur post-loss. After this alignment, only 0.25% of GFW-detected losses occur non-forested land. I drop these GFW-losses from the dataset. However, there remains a set of forest-to-nonforest land use transitions without corresponding GFW-detected loss. I combine these forest loss events with the GFW forest loss variable to create my final forest loss measure. Doing so adds an extra 12% more loss events compared to the original GFW loss measure alone.

Following the harmonization of land use and forest loss, I next align aboveground biomass data to be consistent with these two datasets. The core reason for temporal discrepancies here is two-fold. First, biomass measurements are based on dense Landsat image stacks throughout the entire calendar year. Therefore, a loss occurring mid-year will be reflected in the data as the average of biomass pre- and post-loss. Second, the machine learning method used to generate the biomass measure in Kennedy et al., 2018, uses LandTrendr based statistics which in practice smooth biomass estimates across years. In the dataset, this causes biomass to fall prematurely preceding loss events. To correct both of these issues, I update biomass for observations preceding loss events. Specifically, for a measured forest loss occurring at time t , I calculate pre-loss biomass, biomass_t , from year $t - 2$. This is implemented in the following way. First, I update $\text{biomass}_{t-1} = \text{biomass}_{t-2} * (1 + g(\text{biomass}_{t-2}))$, for all loss events

where $\text{biomass}_{t-1} < \text{biomass}_{t-2} * (1 + g(\text{biomass}_{t-2}))$. Then I update biomass_t as $\text{biomass}_t = \text{biomass}_{t-1} * (1 + g(\text{biomass}_{t-1}))$ if $\text{biomass}_t < \text{biomass}_{t-1} * (1 + g(\text{biomass}_{t-1}))$. Here the function $g()$ represents the average biomass growth rate derived from our transition function, applied at the biomass levels biomass_{t-2} and biomass_{t-1} , respectively. In other words, we take the last unbiased measure of biomass as the last true measure of biomass before loss events. We allow this unbiased measure to grow according to our estimated transition function to create the measure of biomass at the time of harvest. As we measure biomass removals from forest loss events as $\text{biomass}_t - \text{biomass}_{t+1}$ and the biomass measure is essentially smoothed over local windows due to the use of Landtrendr, we update $\text{biomass}_{t+1} = 0$ following loss events. Further, by setting $\text{biomass}_{t+1} = 0$ our measure is now consistent with estimates of biomass removals from loss events in the U.S. Forest Inventory Analysis (FIA) ground-truth database. Finally, to align the biomass data with the land use data, I set biomass to 0 for non-forest observations. This ensures only forest biomass is measured. Throughout the biomass cleaning protocol, I use biomass data from 1999 and 2000 to correctly adjust the beginning of the time series for loss events in 2001.

Now that the core datasets measuring loss, biomass, and land use are aligned temporally, I delineate forest loss into clearcut events and natural loss events using attribution data. Specifically, I identify natural loss events using the GFW losses due to fire dataset, which includes high and very high probability codes 3 and 4, and the LCMS attribution dataset, which contains codes for fire, wind, hurricanes, insects, and other natural causes. If a measured loss event is found to coincide with either of these measures, I define that as a natural loss. Then I define clear cuts as forest loss events that are not natural loss. In the US South, risk from fire, pests, and wind are considered to be relatively low and this is confirmed in our data where approximately 98% of measured forest loss events are categorized as clearcut events.

In summary, this data alignment procedure produces our key measures for: land use, clear cuts, natural losses, and above-ground biomass. Finally, I define forest planting events as occurring in the year where land use transitions from non-forest to forest. Replanting events are defined to happen the year following a forest loss for all plots which remain forested post-loss.

A.2. Mill Dataset Creation

The mill dataset is created from five data sources. First, the core dataset of mill locations, entry and exit dates, ownership, and feedstock wood type comes from the Forisk Mill Capacity Database and covers 2009 to 2023. I then extend this series backwards to the year 2000 using 4 data sources, each covering a different mill type.

For sawmills, I utilize a series of reports produced by the USFS between 1995 and 2009 (Spelter and McKeever, 1999; Spelter and Alderman, 2005; Spelter et al., 2009). These reports provide data on mill locations, entry and exit dates, and ownership of all sawmills in the region. I use the overlap in 2009 data to ensure consistency. The USFS data do not include precise geographic coordinates for each mill but instead report the city, state, and firm name. These attributes are sufficient to reliably match mills across datasets. A small subset of sawmills, representing fewer than two percent of the sample, could not be matched automatically. For these mills, entry and exit dates as well as ownership histories were manually verified using company records and historical imagery from Google Earth. All mill matches and verification details were rigorously validated to ensure accuracy and consistency across datasets.

For pulp mills, I use annual USFS Southern Pulpwood Production from 2000 to 2009, which provide information on mill locations, annual capacities, and ownership. Mill entry and exit are inferred from additions to and removals from these annual lists. Every pulp mill in Forisk is matched directly between datasets (Johnson and Steppleton, 2002, 2011). For OSB mills, a type of wood-receiving mill, I confirm entry dates using data from a report from Forest2Market (2015) which provides data on mill presence for this class of mill from 1995-2010. Finally, for pellet mills, I use data from the Southern Environmental Law Center, to pin down entry dates for the set of pellet mills active in the Forisk prior to 2009 (Sackett, 2023).

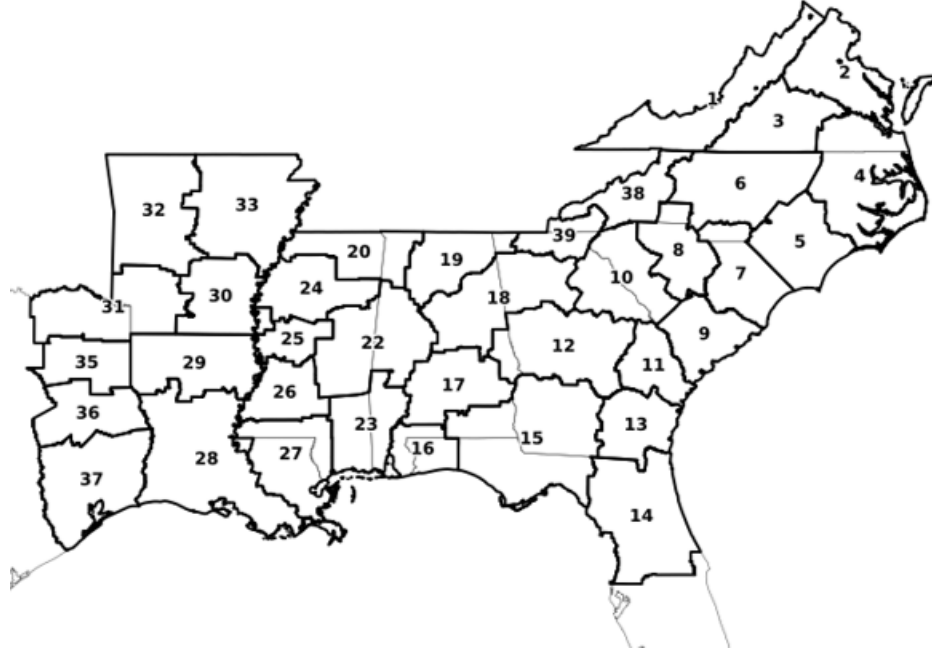
Now I have a complete time series of capacities for each mill type from 2000 to 2023. Next I harmonize capacity measures across mill types to be in the same units: tons of wood demanded at capacity. This measure is provided in the Forisk dataset and is stable within a mill type for a given source wood type (softwood or hardwood). The table below gives the conversion factors used in the paper to convert each mill types original capacity measures into the same units.

After combining these sources, I obtain a complete panel dataset of mill locations, ownership, and feedstock wood type for all wood-processing facilities from 2000 to 2023. Using this dataset, I construct local market structure measures for each sampled plot. Specifically, I compute $N^{w,d}$, where w denotes the dominant wood type processed by the mill (softwood or hardwood) and d represents the distance radius. For each plot producing wood of type w , $N^{w,d}$ measures the number of unique mill owners operating any mill that processes wood of type w within distance d of that plot. This measure effectively captures the number of potential bidding mills a landowner could expect at auction. Mills that process both hardwood and softwood are included for plots producing either wood type.

A.3. Markets & Prices

Prices are provided by Forest2Market for each 33 wood purchasing markets in the study region. Forest2Market defines a wood purchasing market (a micro-market in their dataset) using transaction level data between mills and landowners to define 'typical' market boundaries. Each county is then assigned to a given market. In practice, there are about 2-3 markets per state, although markets do not necessarily conform to state boundaries. For each market, there are four price series. One for each wood-type and grade (i.e. sawtimber or pulpwood for each of hardwood or softwood). Figure A.2 shows the market boundaries for the set of markets in the study area. For each plot, we then assign the annual product prices, based on the geographic market the plot is located within and the wood type the plot is assigned from the Williams et al. (2020) dataset. Saw prices are shown below, where all prices are indexed such that the mean price across all softwood markets in 2000 is 100.³⁵

Figure A.1: F2M Market Definitions

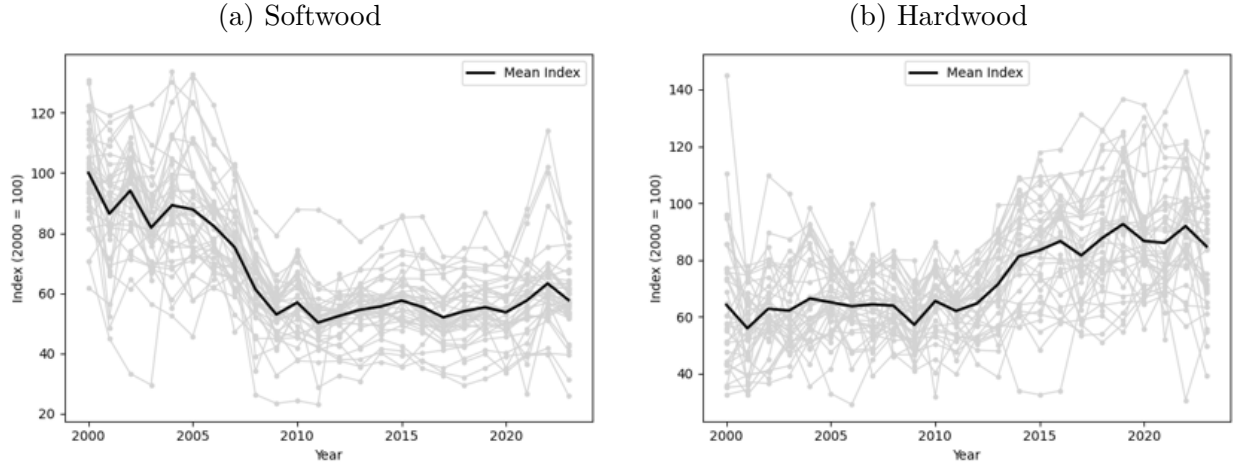


A.4. Biomass to Wood Products (α function estimation)

In the paper, I take a given stock of aboveground biomass observed at time t and apply two functions to determine the share of biomass that is sawtimber or pulpwood on each site. These share functions, $\alpha^{\text{saw}}(b_{it})$ and $\alpha^{\text{pulp}}(b_{it})$, are estimated from the ground-truth plot-level

³⁵This is a requirement of the data vendor.

Figure A.2: Sawlog Prices, U.S. South Wood Markets



data of the USFS Forest Inventory and Analysis (FIA) program for each state in the study area. The FIA dataset is particularly advantageous because the biomass measure is the same ground-truth data used in Kennedy et al. (2018) to calibrate satellite-based biomass estimates.

The FIA plots are 1/6-acre in size, revisited roughly every five years, and spaced approximately 5.5 km apart. At each visit, field crews measure for each tree the total above-ground biomass and the portions allocated to sawtimber, pulpwood, and residual biomass (i.e., bark, branches, leaves, and stump). Tree species are also recorded and classified. Using these data, I classify plots as hardwood or softwood by the most dominate single forest type. Given the small size of a plot, most are homogeneous. For each plot, I aggregate tree-level biomass components to the plot level, then estimate α^{saw} and α^{pulp} functions separately for hardwood and softwood plots.

For estimation, I employ a modified Chapman–Richards growth model following Barnett et al. (2023). The functional form is:

$$\alpha_i = \theta_1 \left(1 - e^{-\theta_2 b_i}\right)^{\theta_3} + \varepsilon_i,$$

where b_i is total above-ground biomass for plot i , θ_1 represents the asymptotic (maximum) share of sawtimber (or pulpwood) as biomass increases, θ_2 governs the rate of increase, and θ_3 controls the inflection and curvature of the relationship. The parameters are estimated using nonlinear least squares separately for sawtimber and pulpwood shares within hardwood and softwood plots.

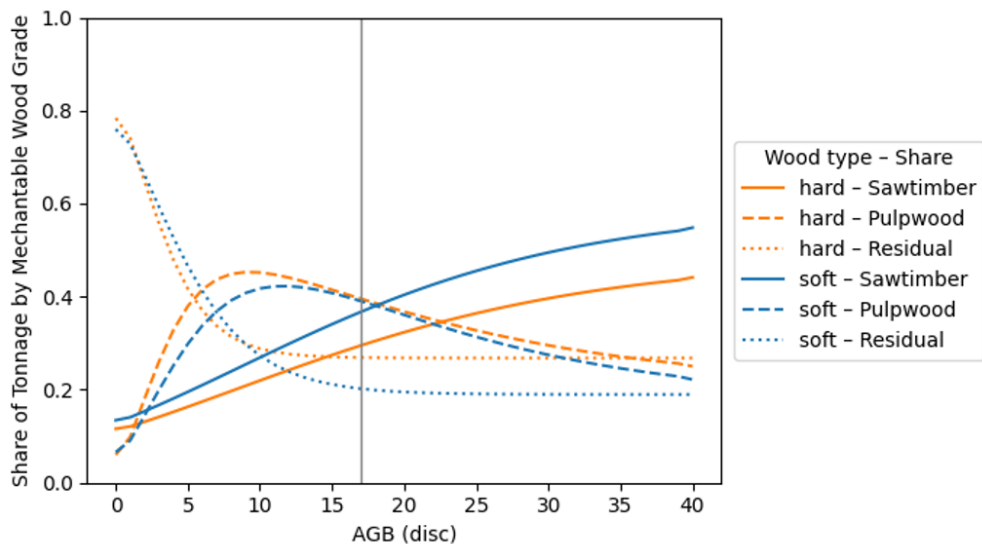
Although most forestry growth models relate biomass or volume to stand age, modeling composition shares as a function of biomass density is equally appropriate, since the accumulation of sawtimber and pulpwood follows similar sigmoidal dynamics. The modified Chapman–Richards specification provides a biologically realistic, flexible functional form for these relationships (Barnett et al., 2023). Table A.2 reports the estimated model results and shows that there is strong goodness-of-fit across all four models, and Figure A.2 shows the predicted share curves along with the implied share of residues.

Table A.2: Chapman–Richards Growth Estimates

	Softwood		Hardwood	
	Sawtimber	Pulpwood	Sawtimber	Pulpwood
θ_1	0.591*** (0.0044)	0.770*** (0.0009)	0.482*** (0.0020)	0.692*** (0.0006)
θ_2	0.449*** (0.0127)	0.568*** (0.0098)	0.499*** (0.0093)	0.549*** (0.0102)
θ_3	0.014*** (0.0003)	0.051*** (0.0005)	0.013*** (0.0002)	0.077*** (0.0008)
R^2	0.827	0.972	0.871	0.967

Notes: Standard errors in parentheses. *, **, *** denote significance at the 10%, 5%, and 1% levels respectively.

Figure A.3: Estimated shares by biomass level



B. Estimation

Table A.2 reports the estimated autoregressive parameters for sawtimber and pulpwood prices by wood type. All series are estimated using the Blundell–Bond two-step system GMM estimator (Blundell and Bond, 1998) with market fixed effects which account for price differences across markets. The instrument set uses lagged levels (from $t!-12$ and earlier) and first differences (from $t!-1$ and earlier) of prices as instruments. The results confirm strong persistence in log prices, with autoregressive coefficients ranging from 0.89 to 0.92 for softwood and 0.41 to 0.56 for hardwood. The Hansen test statistics indicate no evidence of instrument overidentification at conventional significance levels. These results validate the AR(1) assumption used in the construction of the discrete price transition matrices described in Section 6.

Table B.1: AR(1) Estimates for Prices by Wood Type and Grade

	Softwood		Hardwood	
	Sawtimber	Pulpwood	Sawtimber	Pulpwood
Lagged Price	0.919*** (0.0129)	0.891*** (0.0452)	0.559*** (0.0566)	0.411*** (0.0720)
Constant	0.203*** (0.0417)	0.195*** (0.0965)	1.430*** (0.186)	1.125*** (0.149)
Hansen Test Statistic	39.00	37.74	38.90	27.40
(p-value)	0.603	0.658	0.608	0.197

Notes: Standard errors in parentheses. *, **, *** denote significance at the 10%, 5%, and 1% levels respectively.

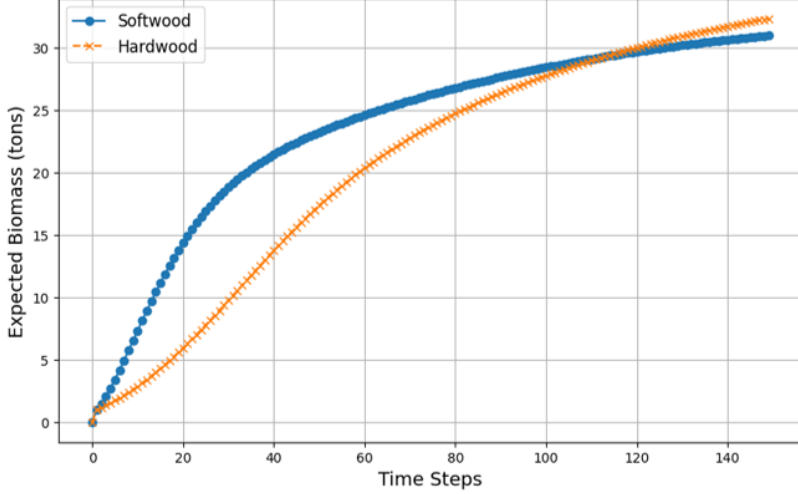
Figure 15 presents the simulated biomass growth trajectories implied by the estimated Markov transition functions, beginning from an initial biomass level of zero and projected forward for 150 years. Each curve represents the expected evolution of aboveground biomass under the estimated transition process for softwood and hardwood stands.

Softwoods exhibit much faster early growth, with expected biomass accumulation leveling off after roughly 100–120 years. Hardwoods grow more slowly but ultimately achieve a higher asymptotic biomass level. This pattern aligns with biological and silvicultural expectations: softwood species mature rapidly and are typically harvested sooner, while hardwoods exhibit slower growth and higher eventual volume.

As the modal biomass level at harvest is 17 tons for both forest types, these growth

functions align well with standard harvesting timelines. Standard practice in the region is to harvest softwoods when trees reach 25-30 years, and hardwoods when they reach 50-60 years old. These growth curves show that the modal level of harvest is achieved at 25 years for softwoods, and 49 years for hardwoods. Thus these growth curves are consistent with industry-standard harvest cycles observed in the U.S. South.

Figure B.1: Simulated Biomass Growth



C. Mill Dynamics After Pellet Entry

The counterfactuals in the paper remove pellet mills from the potential bidder set. Absent an explicit entry-exit model, this may misspecify their impact on market structure. Pellet mills both compete with other fiber-consuming mills (e.g., pulp, plywood) and purchase residues from sawmills, potentially inducing exit of the former and entry of the latter. To study these dynamics, I construct mill counts for each F2M market by summing the number of operating mills in each year, by mill type (sawmill, pulp, etc.) and wood type (hardwood or softwood). To ensure pellet mills are not simply new facilities opened by incumbents, I also examine whether the number of unique firms changes.

I frame the analysis in terms of the following event-study specification:

$$N_{mt}^j = \alpha_m + \gamma_t + \sum_{k=-K}^K \beta_k \mathbf{1}\{t - T_m = k\} + \varepsilon_{mt}, \quad (2)$$

where N_{mt}^j is the number of mills of type j in market m and year t , while α_m and γ_t are two-way fixed effects.

Although equation (2) provides the canonical regression equation, I estimate the dynamic treatment effects β_k using the staggered-adoption difference-in-differences estimator of Callaway and Sant'Anna (2021). This approach recovers group-time average treatment effects relative to the not-yet-treated sample, which I then aggregate into event-study coefficients. In practice, this avoids the bias that arises in traditional two-way fixed effects regressions under staggered treatment timing.

Markets are treated in the year a pellet mill begins operations, T_m , with adoption occurring at different times across markets. By 2023, 16 markets experience a softwood pellet entry and 13 experience a hardwood pellet entry.

Table A3 summarizes the results. As expected we see that the number of pellet mills increases with treatment, with point estimates exceeding one indicating that on average more than one pellet mill enters. Coefficients for sawmills and other fiber consuming mills are in the expected direction, but statistically insignificant. The exception is hardwood sawmills, where results suggest that pellet mills induced sawmill entry, though this result is only marginally statistically significant. In light of this, my counterfactuals can be thought of as a lower bound on the change in the potential bidder set. In other words, if sawmill entry were properly accounted for, the change in the potential bidder set would be larger. Finally, the increase in number of unique firms in treated markets illustrates that pellet mills were not established by incumbent firms.

Table C.1: Treatment Effects on Mill Counts and Competition by Wood Type

	Pellet Mills	Sawmills	Other Pulp Mills	Bidders
Softwoods				
ATT	1.355*** (0.183)	0.052 (0.226)	-0.112 (0.128)	1.342*** (0.222)
Hardwoods				
ATT	1.370*** (0.401)	0.224* (0.135)	-0.135 (0.149)	1.105*** (0.171)

Notes: Standard errors in parentheses. *, **, *** denote significance at the 10%, 5%, and 1% levels respectively.

D. Long-Run Simulations

In this appendix, I extend the counterfactual simulations forward by 250 years to show the long-run dynamics implied by the model. These long-run results show that forest biomass approaches a steady state around the year 2250. Over this horizon, the forest stock with pellet mills remains permanently lower than in the no-pellet counterfactual. Carbon sequestration remains reduced over the entire 250-year span, indicating a persistent weakening of the carbon land sink. Forest loss continues throughout the simulation, reaching roughly 12,000 km² of additional loss after 250 years, larger than the urban area of every U.S. city. The underlying mechanism remains the same as in the main analysis: increased harvests combined with incomplete replanting accelerate the conversion of forest land. However, these long-run projections show that while deforestation rates level off by around 2250, afforestation continues to gradually rise, suggesting a slow approach toward a new equilibrium in which total forest area remains permanently lower.

It is important to emphasize that extending the model so far into the future assumes the underlying land-use processes remain stable, including the gradual net deforestation trend observed in the data. Over such a long horizon, many factors could alter these dynamics: technological change in forest management, shifts in land policy, evolving urban expansion pressures, or new carbon mitigation instruments. The current simulation should therefore be interpreted as a stylized projection conditional on present mechanisms persisting. Within that framework, the results highlight that the policy primarily amplifies an ongoing process of net deforestation, rather than introducing a new one, and that this acceleration has lasting implications for the long-run forest area, biomass, and carbon storage.

Figure D.1: Long Run Biomass & Carbon

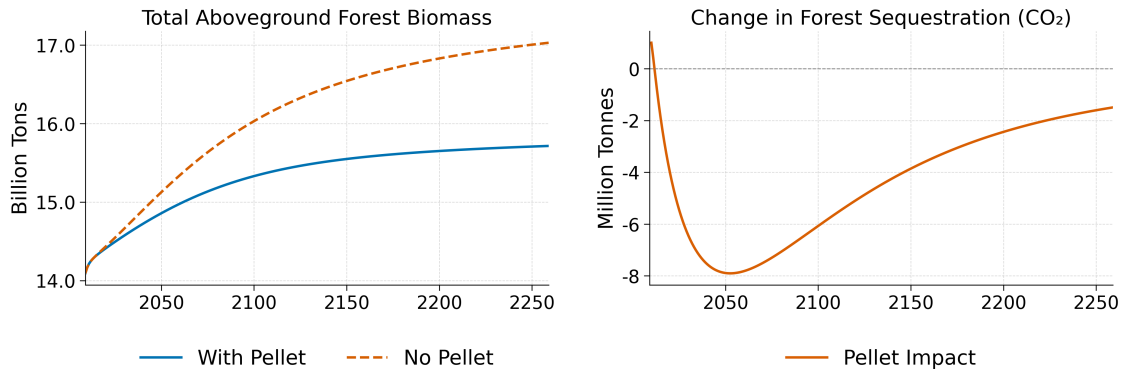
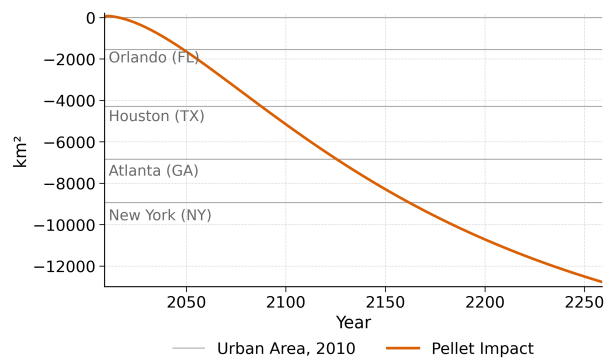
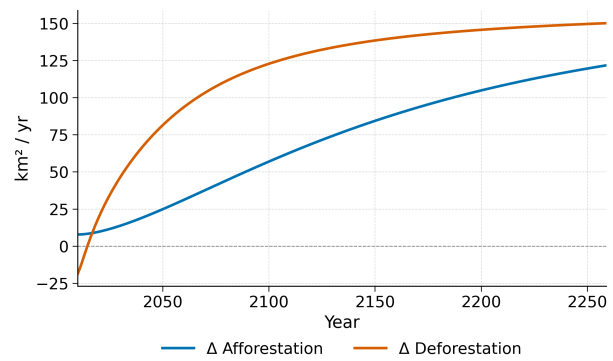


Figure D.2: Long Run Forest Loss



(a) Net Forest Loss



(b) Afforestation vs. Deforestation